

# Machine Learning-Driven Correction of Handgrip Strength: A Novel Biomarker for Neurological and Health Outcomes in the UK Biobank

Kimia Nazarzadeh<sup>1,2,3\*</sup>, Simon B. Eickhoff<sup>2,4</sup>, Georgios Antonopoulos<sup>2,4</sup>, Lukas Hensel<sup>1</sup>, Caroline Tschempel<sup>1,5</sup>, Vera Komeyer<sup>2,4,6</sup>, Federico Raimondo<sup>2,4</sup>, Veronika Müller<sup>2,4</sup>, Christian Grefkes<sup>5</sup>, Kaustubh R. Patil<sup>2,4\*</sup>

## Abstract

**Background:** Handgrip strength (HGS) is a significant biomarker for overall health, offering a simple, cost-effective method for assessing muscle function. Lower HGS is linked to higher mortality, functional decline, cognitive impairments, and chronic diseases. Considering the influence of anthropometrics and demographics on HGS, this study aims to develop a corrected HGS score using machine learning (ML) models to enhance its utility in understanding brain health and disease.

**Methods:** Using UK Biobank data, sex-specific ML models were developed to predict HGS based on three anthropometric variables and age. A novel biomarker,  $\Delta HGS$ , was introduced as the difference between true HGS (i.e., directly measured HGS) and bias-free predicted HGS. The neural basis of true HGS and  $\Delta HGS$  was investigated by correlating them to regional gray matter volume (GMV). Statistical analyses were performed to test their sensitivity to longitudinal changes in stroke and major depressive disorder (MDD) patients compared to matched healthy controls (HC).

**Results:** HGS could be accurately predicted using anthropometric and demographic features, with linear support vector machine (SVM) demonstrating high accuracy. Compared to true HGS,  $\Delta HGS$  showed high reassessment reliability and stronger, widespread associations with GMV, especially in motor-related regions. Longitudinal analysis revealed that neither HGS nor  $\Delta HGS$  effectively differentiated patients from matched HC at post time-point.

**Conclusion:** The proposed  $\Delta HGS$  score exhibited stronger correlations with GMV compared to true HGS, suggesting it better represents the relationship between muscle strength and brain structure. While not effective in differentiating patients from HC at post time-point, the increase in  $\Delta HGS$  from pre to post time-points in patient cohorts may indicate improved utility for monitoring disease progression, treatment efficacy, or rehabilitation effects, warranting further longitudinal validation.

**Keywords:** machine learning, handgrip strength, stroke, depression, UK Biobank, structural MRI

## Background

Handgrip strength (HGS) is broadly recognized as a reliable and non-invasive biomarker of overall health. It is typically measured isometrically using a hydraulic hand dynamometer, an instrument that shows good reassessment reliability [1,2]. This measurement involves participants squeezing the dynamometer with maximum effort without any hand or arm movement, thus measuring the isometric grip force. Direct measured HGS offers several advantages, including low cost, ease of administration, and a strong predictive value for various health outcomes [1,3–6]. Beyond, HGS is related to the grey matter volume (GMV) of the brain, which in turn has been used as a marker for neuropathological changes in neurodegenerative and psychiatric diseases. GMV has also been associated with protective factors such as muscular strength [1]. Lower GMV is associated with lower HGS [7]. On the other hand, stronger HGS is associated with higher GMV in a wide array of brain regions like the ventral striatum, hippocampus, thalamus, pallidum, putamen, brain stem, temporal pole, and parahippocampal gyrus [1]. Through its associations with physical capabilities and with structural brain integrity, HGS offers insights into the neurobiological mechanisms related to muscle strength [1]. This relationship, however,

**NOTE: This preprint reports new research that has not been certified by peer review and should not be used to guide clinical practice.**

\* Correspondence: Kimia Nazarzadeh; Kaustubh R. Patil

<sup>1</sup> Department of Neurology, Faculty of Medicine, University Hospital Cologne, University of Cologne, Cologne, Germany

<sup>2</sup> Institute of Neuroscience and Medicine, Brain & Behaviour (INM-7), Research Centre Jülich, Jülich, Germany

Full list of author information is available at the end of the article.

47 is influenced by genetics, physical fitness, mental health as well as anthropometrics, and demographic  
48 characteristics, emphasizing the need for a comprehensive examination of these associations [1].

49 HGS serves as a marker of overall health because it can be affected through different mechanisms.  
50 Lower HGS in older adults is associated with adverse health outcomes, such as increased mortality risk,  
51 diminished functional mobility, cognitive impairments, and a range of health issues, including  
52 metabolic diseases like diabetes, and neurological conditions including stroke and major depressive  
53 disorder (MDD) [8–10]. Moreover, reduced HGS is not only linked to higher disease recovery times  
54 [11] but also functions as a valuable biomarker for assessing recovery and prognosis in stroke patients,  
55 with evidence linking a decrease in HGS after stroke (post-stroke) compared to before stroke (pre-  
56 stroke) levels [12,13]. These attributes have established HGS as an indicator of muscle strength and  
57 general health in clinical settings [1,8,11,14]. While understanding longitudinal changes in HGS in  
58 patients can help risk assessment and improve monitoring, to date it remains understudied due to lack  
59 of longitudinal data.

60 Anthropometric factors such as height, body mass index (BMI), and waist-to-hip ratio (WHR) are  
61 directly linked to HGS [15–20]. For instance, BMI and height correlate positively with greater strength  
62 [17,19]. Conversely, WHR, which reflects the proportion of abdominal fat relative to hip circumference,  
63 often exhibits an inverse relationship with HGS. Greater abdominal fat relative to hip size is frequently  
64 associated with lower HGS [18]. Age is another critical factor affecting HGS. Generally, HGS increases  
65 during childhood and adolescence, peaks in early adulthood, and then declines with higher age,  
66 particularly after 40. This decline is often more pronounced in older adults, especially those over 75,  
67 where the rate of decrease accelerates [16]. The aging process results in progressive muscle loss, further  
68 impacting HGS [16], [21]. Sex differences also contribute significantly to variations in HGS [22,23],  
69 influencing both baseline strength levels and decline patterns. Males and females exhibit distinct  
70 patterns in disease progression and anthropometric measurements, necessitating sex-specific  
71 considerations in clinical and research settings [24]. The interpretation of HGS is thus most meaningful  
72 when normalized to anthropometric and demographic factors, rather than relying on raw measured  
73 values. Relative HGS, which accounts for these variables, may offer a more precise assessment of an  
74 individual's neuromuscular deficit and its relationship with brain structure and diseases, potentially  
75 improving its utility as a health indicator [8,11,12,25]. In particular, a refined HGS interpretation can  
76 open up new possibilities for early disease detection, monitoring treatment efficacy, guiding recovery  
77 processes, and predicting long-term health outcomes across various conditions.

78 Machine learning (ML) based predictive modelling offers individual-level predictions, establishing  
79 ML as a transformative tool in modern clinical practice [20,26]. ML can be used to predict HGS using  
80 anthropometric and demographic features. This predicted HGS captures the variance explained by the  
81 features and thus can be used to develop a relative HGS score. In this study, we tested the hypothesis  
82 that the difference between true HGS and predicted HGS can serve as a biomarker for muscular strength  
83 relating to the structural integrity of the brain and disease-related changes. Using data from the UK  
84 Biobank (UKB), we developed sex-specific ML models to predict HGS using anthropometrics and  
85 demographic variables in healthy individuals. We applied statistical bias-correction techniques to  
86 enhance prediction accuracy and introduced a novel score called  $\Delta HGS$ , defined as the difference  
87 between the true HGS and bias-free predicted HGS. We then investigated the brain basis  $\Delta HGS$  based  
88 on correlation with regional GMV followed by the investigation of its sensitivity to longitudinal changes  
89 in patient cohorts from two diseases known to influence HGS: stroke and MDD. The key innovation  
90 lies in our longitudinal design, capturing HGS scores at two time points: before (pre) and after (post)  
91 disease onset. This approach enabled us to examine how  $\Delta HGS$  and true HGS change over time in  
92 patients compared to healthy controls (HC) groups.

93  
94

## Methods

### Participants and data

We used data from the UK Biobank database with more than half a million adult participants recruited from a total of 22 assessment centers across the United Kingdom (UK) with baseline assessment between 2006 and 2010. The baseline assessment included a wide range of demographic data, physical measurements, clinical and health-related information, and the completion of a touchscreen questionnaire [27,28]. A subset of participants was invited back in 2012-2013 for the first repeat assessment. During this repeat visit, additional data were collected, although no brain imaging data were collected at either the baseline or the first repeat assessment. Starting in 2014, a subsample was invited to assessment centers for brain imaging, with follow-up imaging assessments beginning in 2019. In this study, participants were categorized into three groups: healthy controls (HC) and two patient cohorts: stroke and MDD. Group definitions were established using inclusion and exclusion criteria based on the International Classification of Diseases, 10th revision (ICD-10) coding system. We required that all anthropometrics, demographics, and HGS be complete for each participant in the final study sample to ensure no missing values (Fig. 1).

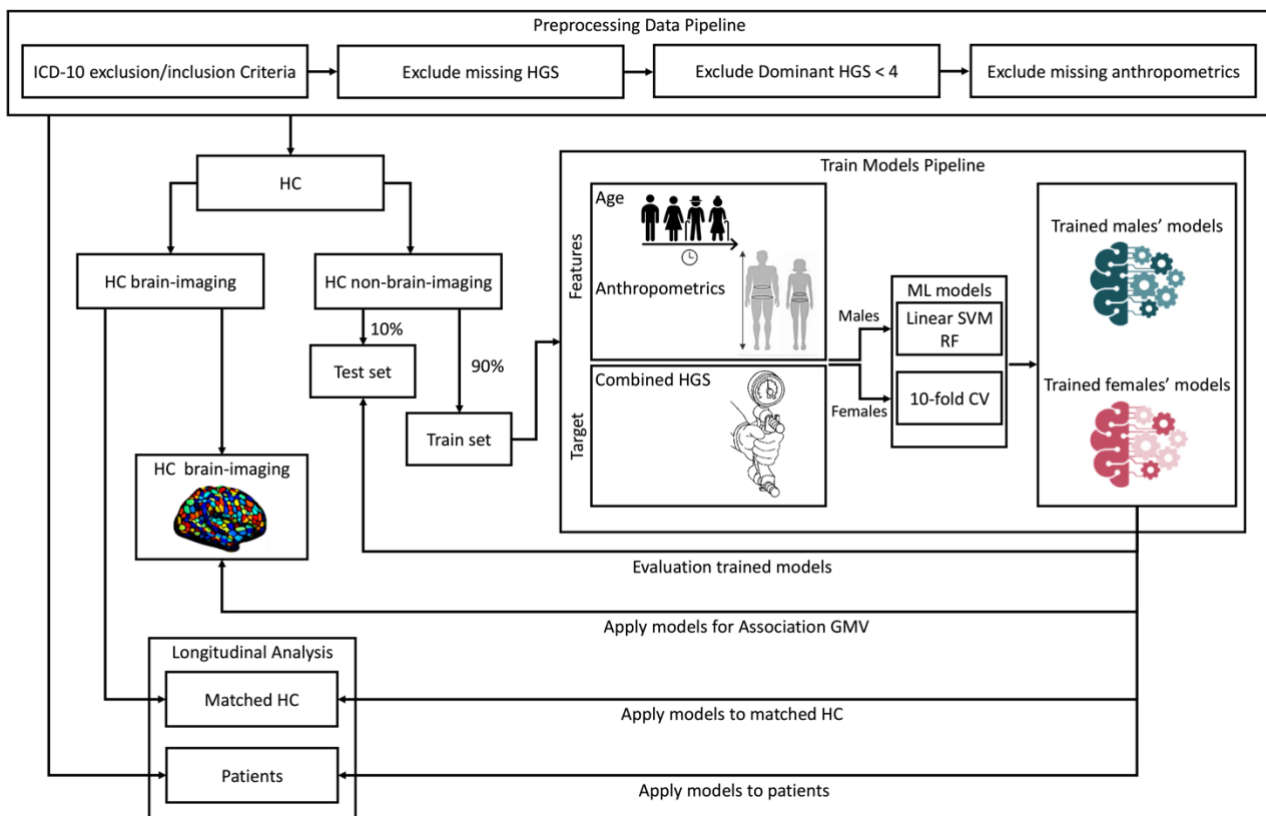


**Fig. 1** The ML analysis pipeline used to predict HGS and analyze its associations with neurobiological markers and disease-related impairments in this study. For data preparation anthropometric (BMI, height, and waist-to-hip ratio) and demographic (age) variables were obtained from the UK Biobank database. These variables (predictors) were used to train sex-specific ML models, specifically linear SVM and random forest (RF), to predict HGS. The pipeline includes steps for preprocessing, model training, performance evaluation through cross-validation, and the application of statistical bias-correction techniques to enhance prediction accuracy. The true HGS and  $\Delta HGS$  (true HGS -  $HGS^c$ ; see the “Model training and performance evaluation” section) scores are then assessed for their correlation with neurobiological markers, such as gray matter volume (GMV), and their effectiveness in distinguishing between HC and patients with stroke and MDD.

123 **Table 1** Definition of the study populations based on ICD-10 criteria for HC, stroke, and MDD

Populations	Excluded ICD-10 criteria	Included ICD-10 criteria
Healthy controls (HC)	Mental and behavioural disorders: F Diseases of the nervous system: G Cerebrovascular diseases: I60-I69 Diseases of the musculoskeletal system and connective tissue: M Injury, poisoning, and certain other consequences of external causes: S	-
Stroke	Mental and behavioural disorders: F Diseases of the nervous system: G00-G14, G20-G26, G30-G32, G35-G37, G54-G59, G60- G61, G70-G73, G80-G83, G91-G99 Diseases of the musculoskeletal system and connective tissue: M Injury, poisoning, and certain other consequences of external causes: S	Ischemic: I63 Intracerebral haemorrhage: I61
Major depressive disorder (MDD)	Mental and behavioural disorders: F00-F31, F34-F48, F50-F99 Diseases of the nervous system: G Cerebrovascular diseases: I60-I69 Diseases of the musculoskeletal system and connective tissue: M Injury, poisoning, and certain other consequences of external causes: S	Depressive episode: F32 Recurrent depressive disorder: F33

124

125

### 126 **Healthy controls**

127 The HC population was obtained by excluding participants with a known history or current diagnosis  
128 of mental and behavioral, psychiatric, nervous system, neurological, cardiovascular, cerebrovascular,  
129 musculoskeletal system, connective tissue conditions, injuries or poisoning diseases as outlined in the  
130 ICD-10 codes (Table 1). The HC participants were divided into two groups: 1) participants who did not  
131 undergo brain imaging assessments (non-imaging data,  $N = 201,133$ ) and 2) participants who  
132 participated in at least one brain imaging assessment out of the two available imaging assessments (HC  
133 with imaging data,  $N = 32,125$ ). Individuals with non-imaging data were used to train and evaluate ML  
134 models. The HC individuals with imaging data were employed both in assessing the association between  
135 HGS and GMV as well as for matched HC comparisons with patient cohorts (Additional file 1: Figure  
136 S1).

137

138

### 139 **Patient cohorts**

140 First, participants with conditions of the musculoskeletal system, connective tissue, or injury were  
141 excluded from all patient sample groups (Table 1). The outcomes of incident stroke were defined  
142 according to the “algorithmically-defined outcomes (ADOs)” (UKB Resource 460) developed by the  
143 UKB team [29]. The algorithm integrated information from UKB’s baseline assessment data collection  
144 along with linkage data, including hospital admissions, diagnoses and procedures, death register  
145 records, and self-reported medical condition codes reported at the baseline assessment visit. The  
146 incident MDD outcome was obtained from “the first occurrence of health outcomes defined by 3-  
147 character ICD-10 code” algorithm (UKB Resource 593) [30,31]. The UK Biobank indicated the first  
148 occurrence of a set of diagnostic codes for a wide range of health outcomes across self-report, primary  
149 care, hospital inpatient data, and death data, mapped to a 3-digit ICD-10 code. To establish patient  
150 cohorts, we included stroke endpoints comprised of ischemic stroke (I63) or intracerebral hemorrhagic  
151 stroke (I61), and MDD depressive episode (F32) or recurrent depressive disorder (F33). The onset dates  
152 for the diagnoses of two diseases were identified using the first occurrence fields: stroke (Data-Field  
153 42006), and MDD (Data-Fields 130894 and 130896). To ensure diagnostic accuracy, cases based solely  
154 on self-reported data were excluded from the analysis. Patients with a history of diseases prior to their  
155 baseline assessment visit were excluded to ensure that the analysis focuses on incident cases. Additional  
156 exclusion criteria were applied to each patient group, including missing dates of disease onset, missing  
157 data, and relevant HGS conditions (see the “[Handgrip strength assessment](#)” section). After applying  
158 exclusion criteria, we identified disease cohorts consisting of patients with longitudinal data who

159 completed assessments at two time-points: (1) an initial assessment visit prior to the onset of the disease  
160 (pre time-point), and (2) the first follow-up assessment visit after disease onset (post time-point). The  
161 final patient cohorts comprised: 40 males and 16 females in the stroke group (1 female patient  
162 hemorrhagic and all others ischemic), and 37 males and 60 females in the MDD group. These cohorts  
163 provided longitudinal data for analysis of HGS changes concerning disease onset.

164  
165

### 166 **Handgrip strength assessment**

167 HGS was measured isometrically using a calibrated Jamar J00105 hydraulic hand dynamometer  
168 (Lafayette Instrument Company, USA), which was monitored by a research assistant. During the HGS  
169 measurement, participants were told to sit upright in a chair with their forearms resting on armrests  
170 pointing forward and their elbows bent and locked at a 90° angle. The maximum HGS value was  
171 obtained from each hand while participants were instructed to squeeze the handle as hard as possible  
172 for approximately 3 seconds. Both hands were measured consecutively (Data-Field 46 for the left and  
173 Data-Field 47 for the right hand). Participants whose dominant HGS < 4 kg or lower than their non-  
174 dominant HGS were eliminated from further analysis [1,32]. Hand dominance was based on self-  
175 report. If information on handedness was not available or if the individual reported using both hands  
176 (ambidextrous) we based dominance on the highest HGS score obtained from either right or left hand.  
177 In this study, our target of interest was combined HGS (which we refer to simply as HGS), calculated  
178 as the sum of the grip strength measurements from the right and left hands. While measuring HGS in  
179 each hand separately can reveal unilateral deficiencies, assessing combined HGS provides a  
180 comprehensive measure of overall hand strength. In clinical settings, assessing the strength of both  
181 hands offers a robust measure of overall strength and helps identify unilateral weaknesses or conditions  
182 affecting one side of the body that may be overlooked with single-hand testing, especially for conditions  
183 like stroke or localized musculoskeletal disorders [33]. This approach is particularly relevant when  
184 considering the 10% rule, which states that the dominant hand typically has a 10% greater grip strength  
185 than the non-dominant hand, primarily applies to right-handed individuals, who make up more than  
186 90% of both male and female participants in this study. In contrast, for left-handed individuals, grip  
187 strength tends to be more balanced between both hands [34]. Therefore, combined HGS offers a more  
188 equitable assessment for left-handed individuals, as it eliminates the need for adjustments based on hand  
189 dominance. Note that for lateralized motor deficits as encountered in stroke, the combined HGS score  
190 will also be reduced.

191  
192

### 193 **Demographic and Anthropometric assessments**

194 Participants' sex was determined from self-reported information (Data-Field 31). Age was calculated  
195 based on the date of the baseline assessment attendance and the participant's birth date. Anthropometric  
196 data were obtained during the physical measures phase of each assessment visit. Height (Data-Field 50)  
197 was directly measured, while BMI (Data-Field 21001) was calculated using weight and height data  
198 (kg/m<sup>2</sup>). WHR was determined by dividing waist circumference (Data-Field 48) by hip circumference  
199 (Data-Field 49).

200  
201

### 202 **ML analysis**

#### 203 **Data preparation**

204 Data from non-imaging HC participants who only attended the baseline assessment was used to train  
205 and evaluate ML models. Age and anthropometric (i.e., BMI, height, and WHR) characteristics were  
206 considered as predictors in our models. To avoid overfitting and base decisions on the most promising  
207 models, we split the HC data into training (90%), and test datasets (10%). The splits were stratified  
208 based on binned age (into 5 bins), HGS (into 5 bins), and sex to keep splits representative of the whole

209 population. After excluding cases with missing data and relevant HGS conditions (see the “Handgrip  
210 strength assessment” section) from each dataset, the final HC data included 61,816 males (43.32%) and  
211 80,886 females (56.68%) in the training set, and 6,938 males (43.62%) and 8,969 females (56.38%) in  
212 the test set (Table 2, Fig. 1, and Additional file 1: Figure S1).

213  
214  
215

**Table 2** Summary of the HC non-imaging population characteristics

Dataset	HC non-brain-imaging at baseline assessment visit					
	Train dataset			Test dataset		
Sex	Both sex	Female	Male	Both sex	Female	Male
Number	142,702	80,886	61,816	15,907	8,969	6,938
Age, mean (SD)	55.46 (8.12)	55.24 (7.99)	55.75 (8.27)	55.54 (8.13)	55.28 (8.01)	55.87 (8.26)
BMI, mean (SD)	26.76 (4.42)	26.35 (4.74)	27.29 (3.91)	26.74 (4.35)	26.29 (4.63)	27.33 (3.89)
Height, mean (SD)	168.46 (9.21)	162.76 (6.27)	175.93 (6.79)	168.47 (9.24)	162.69 (6.24)	175.95 (6.8)
WHR, mean (SD)	0.86 (0.09)	0.81 (0.07)	0.93 (0.06)	0.86 (0.09)	0.81 (0.07)	0.93 (0.06)
Combined HGS, mean (SD)	62.50 (21.27)	48.65 (11.68)	80.62 (16.92)	62.56 (21.25)	48.69 (11.69)	80.48 (16.99)
Right dominant hand	90.34%	91.93%	88.26%	90.16%	91.6%	88.3%

216  
217

### 218 Model training and performance evaluation

219 We utilized the non-imaging HC training dataset (61,816 males and 80,886 females) to train sex-specific  
220 ML models for HGS prediction using the anthropometrics and age features. To prevent sex bias and  
221 given known sex differences in HGS, and anthropometric features, models were trained separately for  
222 males and females. We employed linear support vector machine (SVM) and random forest (RF)  
223 regression models. Our motivation for including a nonlinear predictive model (RF) besides the linear  
224 SVM in our analysis was based on the fact that a non-linear relationship between age and HGS has been  
225 already documented [11,20]. Specifically, HGS generally increases until approximately ages 30 to 40,  
226 after which it begins to decline, and non-linear models are needed to capture such association [35].  
227 Pearson’s correlation coefficient ( $r$ ), the coefficient of determination ( $R^2$ ) and mean absolute error  
228 ( $MAE$ ) were used to compare model performance. To obtain generalization estimates, we performed 10  
229 times repeated 10-fold ( $10 \times 10$ -fold) cross-validation (CV) using the Julearn machine learning library  
230 version 0.2.7 (<https://juaml.github.io/julearn/>) [36], building on top of the scikit-learn library [37]. The

231 hyperparameter  $C$  for the linear SVM was calculated using a heuristic as  $C = 1/\frac{1}{n} \sum_i \sqrt{\sum_j x_{ij}^2}$  where  $n$   
232 is the number of subjects [38]. As an alternative, we also trained a RF regression model using the Scikit-  
233 Learn (sklearn) Python package version 1.2.1, with 100 trees, a minimum of 2 samples per split, the  
234 square root (sqrt) of the total number of features as the maximum number of features considered for the  
235 best split, and bootstrapping of the training samples (true) as the hyperparameters (defaults in this  
236 version of sklearn).

237 In the first step, we performed a scaling study by comparing the prediction performances of both the  
238 linear SVM and RF models across six levels of sample sizes (10, 20, 40, 60, 80, and 100%) generated  
239 by randomly selecting the required number of sampling data from the training dataset to perform the  
240 CV procedure. Comparing model performances across different sample sizes help evaluate model  
241 stability and reliability by revealing how performance changes with increasing amounts of data. The  
242 model with higher performance was selected for further analysis. Feature importance (FI) scores for  
243 each model were derived to quantify the influence of individual feature variables on model outputs. For  
244 the linear SVM model, we used the coefficient parameter (.coef\_) as the FI scores.

245 In the second step, we validated the models trained using the whole training data (90% of HC), by  
246 comparing the true HGS and predicted HGS ( $\widehat{HGS}$ ) values on the 10% hold-out test set. This step is  
247 crucial for determining how well the trained models perform and identifying any inherent biases or  
248 errors in the prediction process. To this end, we calculated the difference between the true HGS and the  
249  $\widehat{HGS}$  (i.e.,  $\Delta \widehat{HGS} = true\ HGS - \widehat{HGS}$ ). A positive  $\Delta \widehat{HGS}$  indicates that the individual is stronger than  
250 expected, while a negative value suggests weaker than expected strength. However, assessing an

251 individual's strength using this difference is highly dependent on the accuracy of the HGS prediction  
252 model. Prediction frameworks often encounter bias, characterized by overestimation of low values and  
253 underestimation of high values in the target variable. Such a bias can compromise model accuracy and  
254 impair the interpretability of predictions on new data [39]. To address this issue and enhance model  
255 performance, we implemented a statistical bias-correction technique, adjusting HGS predictions to align  
256 more closely with the true HGS distribution. We applied the bias-correction method developed by  
257 Beheshti et al. for brain age prediction, given its demonstrated effectiveness in reducing variance [40].  
258 The correction is employed by means of a linear regression model between true HGS and the  $\Delta HGS$ .  
259 We fitted this model using the predictions from out-of-sample validation sets generated through a 10-  
260 fold CV on the training set and calculated the slope ( $\alpha$ ) and intercept ( $\beta$ ) which are used to correct the  
261 predictions to achieve a bias-free HGS value of predicted HGS ( $\widehat{HGS}^c$ ).

$$\widehat{HGS}^c = \widehat{HGS} + (\alpha \times true\ HGS + \beta) \quad (1)$$

262 Like the prediction models, the bias correction models were trained separately for females and males.  
263 Finally, this  $\widehat{HGS}^c$  was subtracted from true HGS:

$$\Delta HGS = true\ HGS - \widehat{HGS}^c \quad (2)$$

264

265

266

### Reassessment reliability

267 We then assessed the agreement between  $\Delta HGS$  values by using the reassessment reliability process in  
268 the subset of HC test dataset. To evaluate the reliability of the selected sex-specific trained models, we  
269 selected participants from the test dataset for which two non-imaging UKB assessment visit sessions  
270 were available: (1) baseline assessment visit as the initial measurement, and (2) first repeat assessment  
271 visit (after 2-7 years) as the reassessment, resulting in 134 males and 162 females for this analysis  
272 (Additional file 1: Table S2). The concordance correlation coefficient (CCC) [41] between  $\Delta HGS$  from  
273 the two assessment visit sessions was calculated. This reassessment reliability analysis was designed to  
274 assess potential changes in relative HGS over time, considering their new age and possible health  
275 changes. The analysis reflects both the stability of scores and their sensitivity to genuine changes in  
276 participant conditions over time, which are crucial factors for interpreting the reliability of outcomes.

277

278

279

### Association between brain structure and HGS scores

#### Imaging data and preprocessing

280 We investigated the neurobiological basis of the HGS scores and their association with GMV. For this,  
281 we utilized MRI data from the UKB's first imaging assessment visit [42], acquired using 3T scanners  
282 following the protocol and acquisition parameters detailed in Miller et al. [43]. The structural  
283 preprocessing of these images was conducted using pipelines developed and executed by the UKB [44].  
284 Specifically, we analyzed the extracted parcel-wise GMV features from T1-weighted (T1w)  
285 preprocessed images. The initial preprocessing of the MRI data involved retrieving T1-weighted  
286 preprocessed images from the UK Biobank, which were then converted into a DataLad dataset for  
287 provenance tracking [45]. Subsequently, voxel-based morphometry was computed using the  
288 Computational Anatomy Toolbox (CAT) version 12.7 resulting in images normalized to the MNI152  
289 space with a 1.5 mm isotropic resolution [46]. The parcel-wise GMV was extracted as the winsorized  
290 mean (with limits set at 10%) of the voxel-wise values per parcel, combining three different brain  
291 atlases: the Schaefer et al. cortical atlas (1000-parcel) [47], the S4 3T version of Tian et al. Melbourne  
292 subcortical atlas (54-parcel) [48], and the cerebellum SUIT Diedrichsen et al. atlas (34-parcel) [49]. The  
293 result was a feature vector containing the parcellated GMV of 1,088 brain regions of interest (ROI) for  
294 each participant. To accommodate for individual differences in total intracranial volume (TIV), we  
295 linearly regressed it out from each brain region. For this analysis, we used a subset of HC participants  
296 who completed the initial imaging visit with 11,077 males and 12,849 females (Additional file 1: Table  
297

298 S1). The final samples were reduced to 7,726 males and 9,292 females based on the availability of all  
299 1,088 GMV features.

300  
301

### 302 **Correlation analysis**

303 We investigated the correlation between the GMV of 1,088 regions separately for true HGS and  $\Delta HGS$ .  
304 The  $\Delta HGS$  values were obtained using the best-performing separate linear SVM models for males and  
305 females (see the “[Model training and performance evaluation](#)” section). Pearson’s  $r$  and corresponding  
306  $p$ -values were computed. To focus on robust associations, we applied a correlation threshold of  $|r| >$   
307  $0.1$  (the absolute values of correlation coefficients exceeding  $0.1$ ) together with correcting  $p$ -values  
308 using the Bonferroni correction with significance determined at  $p_{corrected} < 0.05$ . Separate analyses  
309 were conducted for female and male participants to identify regions significantly associated with each  
310 HGS score. The correlation coefficients for these significant regions were visualized on brain maps for  
311 each sex individually. Additionally, the intersection of the regions showing significance for both sexes  
312 were visualized using averaged correlation coefficients.

313  
314

### 315 **Evaluation of pre-to-post disease longitudinal HGS changes**

#### 316 **Data preparation**

317 We identified patient cohorts with longitudinal data from pre (prior to the disease onset) and post  
318 (follow-up the disease onset) time-points. The  $\Delta HGS$  score could provide insights into disease-specific  
319 variation in HGS between pre and post time-points on longitudinal cases. To investigate this, patients  
320 with diseases were compared with matched HC samples using a 1:10 (case:control) ratio, ensuring  
321 robust comparative analyses. The matching process entailed selecting HC individuals whose assessment  
322 visit sessions at both pre and post time points coincided with those of the patients, thereby maintaining  
323 temporal consistency.

324 The final patient cohorts consisted of 40 males and 16 females with stroke, and 37 males and 60  
325 females with MDD (see the “[Patient cohorts](#)” section). Matched HCs were selected from the pool of  
326 HC participants who had undergone brain imaging assessment visits and were not used in model training  
327 (15,516 males and 16,609 females). Further refinement of subsamples involved excluding data with  
328 missing values and additional HGS conditions (see the “[Handgrip strength assessment](#)” section). The  
329 final number of HC participants included in the matching process for each assessment was as follows:  
330 baseline (11,918 male and 13,714 female), first repeat (1,884 male and 2,013 female), imaging visit  
331 (11,077 male and 12,849 female), and first repeat imaging (1,153 males and 1,359 females). These  
332 refined HC cohorts enabled comprehensive comparisons with patient cohorts across multiple  
333 assessment time points. The HC subsample used in the matched control-case study, categorized by  
334 assessment visit, is detailed in Additional file 1: Table S1. Propensity score matching (PSM) was applied  
335 using a 1:10 nearest-neighbor approach to select HC samples for each patient within each disease cohort  
336 [50]. This method involved matching each patient with 10 HC participants who had similar propensity  
337 scores, taking into account age, anthropometric features at the pre time-point, and the time interval  
338 between pre- and post- assessment visits (days). Finally, post time-point data were identified for each  
339 HC participant to maintain subject consistency between pre and post time-points. This approach ensured  
340 the availability of longitudinal data in the matched HC group, enabling a robust temporal comparison  
341 with the patient cohorts. The matching process was conducted without replacement, ensuring that each  
342 HC individual could be selected as a match only once per patient group (an overlap was allowed of HC  
343 for the different patient samples, i.e., overlaps of HC for stroke and HC for MDD). The characteristics  
344 of the matched HC samples and patients summarized in Table 3.

345  
346



347 **Table 3** Characteristics of matched healthy controls (HC) and patients

Sex Group Time-point	Male				Female			
	Patient		Matched HC		Patient		Matched HC	
	Pre	Post	Pre	Post	Pre	Post	Pre	Post
<b>Stroke</b>								
Number	40	40	400	400	16	16	160	160
Age, mean (SD)	59.65 (6.79)	68.91 (7.95)	59.31 (6.86)	68.24 (7.34)	61.72 (5.08)	71.21 (6.91)	61.29 (5.84)	71.01 (7.34)
BMI, mean (SD)	26.7 (3.23)	25.85 (3.32)	26.68 (3.79)	26.53 (4.02)	26.37 (5.26)	26.7 (5.36)	26.68 (4.71)	26.36 (4.79)
Height, mean (SD)	177.22 (7.23)	176.44 (7.19)	177.34 (6.35)	176.71 (6.51)	162.39 (7.43)	161.3 (7.02)	162.32 (5.89)	161.34 (6.05)
WHR, mean (SD)	0.94 (0.06)	0.94 (0.06)	0.94 (0.06)	0.94 (0.06)	0.82 (0.1)	0.84 (0.1)	0.82 (0.07)	0.84 (0.07)
Combined HGS, mean (SD)	77.55 (16.45)	70.75 (12.9)	80.79 (15.83)	68.84 (16.57)	44.31 (13.03)	44.12 (12.85)	47.08 (11.08)	42.34 (11.4)
Right dominant hand (%)	37 (92.5%)	37 (92.5 %)	359 (89.75%)	359 (89.75%)	16 (100%)	16 (100%)	154 (96.25 %)	154 (96.25 %)
Time to/from disease onset, mean (SD)	-5.14 (2.87)	4.12 (3.28)			-5.71 (3.57)	3.79 (3.13)		
Time elapsed pre- to post- (years)		9.26		8.93		9.5		9.72
<b>MDD</b>								
Number	37	37	370	370	60	60	600	600
Age, mean (SD)	54.9 (6.89)	64.36 (6.82)	55.76 (7.84)	65 (7.77)	52.72 (7.55)	62.02 (7.91)	52.8 (7.53)	62.02 (7.9)
BMI, mean (SD)	27.38 (4.14)	28.21 (4.55)	27.58 (4.05)	27.37 (4.18)	26.01 (3.83)	26.8 (5.03)	26.04 (4.8)	26 (5.07)
Height, mean (SD)	176.02 (6.14)	175.49 (6.16)	176.13 (6.44)	175.7 (6.57)	163.01 (5.09)	162.45 (4.99)	163.28 (6.27)	162.8 (6.3)
WHR, mean (SD)	0.93 (0.05)	0.97 (0.05)	0.93 (0.06)	0.94 (0.07)	0.79 (0.06)	0.82 (0.07)	0.79 (0.06)	0.81 (0.07)
Combined HGS, mean (SD)	78.89 (14.48)	72.59 (14.06)	82.44 (16.04)	70.77 (17.06)	49.98 (12.01)	45.48 (12.2)	53.16 (11.41)	43.73 (11.91)
Right dominant hand (%)	34 (91.89%)	34 (91.89%)	328 (88.65%)	328 (88.65%)	56 (93.33%)	56 (93.33%)	573 (95.5%)	573 (95.5%)
Time to/from disease onset, mean (SD)	-5.78 (3.35)	3.69 (2.6)			-5.26 (3.38)	4.04 (3.13)		
Time elapsed pre- to post- (years)		9.46		9.24		9.3		9.22

348

349

350

## Statistical analysis

351

352

353

354

355

356

357

358

359

360

361

362

363

364

365

366

367

368

369

## Results

370

### HGS predictive modelling

371

372

373

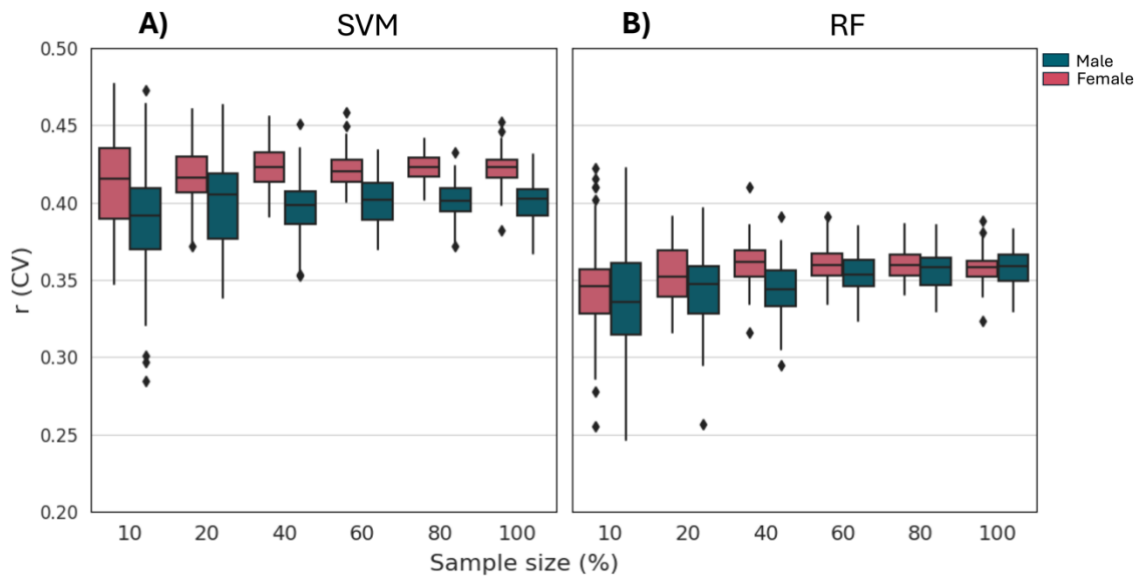
374

375

376

377

We found that HGS can be predicted using both machine learning models, i.e., linear SVM and RF. However, the linear SVM outperformed RF across all sample sizes, achieving higher performance metrics measured as Pearson's correlation coefficient ( $r$ ),  $R^2$ , and MAE for both male and female cohorts (Fig. 2, Table 4). Both models showed a decrease in variance with increasing sample size, as expected. The average performance stabilized after using 40% of the data indicating that the sample size used is large enough to capture the predictive signal adequately.



378

379 **Fig. 2** Pearson correlation coefficient ( $r$ ) from CV analysis at different sample sizes. **A)** linear SVM and **B)** RF models built on the training  
 380 dataset with increasing sample sizes (10% to 100%). The sample size indicates the percentage of data used for performing CV. In males,  
 381 SVM achieved a maximum median  $r$  of 0.405 and  $R^2$  of 0.163 compared to the RF's 0.347 and 0.096 at 20% of the sample size ( $N =$   
 382 12,364). In females, SVM had a maximum median  $r$  of 0.423 and  $R^2$  of 0.179 compared to the RF's 0.359 and 0.107 at 80% of the sample  
 383 size ( $N = 64,712$ ).

384

385

386

**Table 4** Comparison of linear SVM and RF models by increasing sample size on the training dataset

Sex	Models	Scores	Sample sizes					
			10%	20%	40%	60%	80%	100%
Female			$N = 8,089$	$N = 16,178$	$N = 32,356$	$N = 48,534$	$N = 64,712$	$N = 80,886$
	SVM	Pearson	0.415	0.416	0.423	0.420	0.423	0.423
		$R^2$	0.171	0.173	0.178	0.176	0.179	0.178
		MAE	8.441	8.423	8.388	8.384	8.387	8.391
	RF	Pearson	0.346	0.352	0.361	0.360	0.359	0.358
		$R^2$	0.090	0.101	0.108	0.108	0.107	0.107
MAE		8.827	8.757	8.730	8.716	8.730	8.759	
Male			$N = 6,182$	$N = 12,364$	$N = 24,728$	$N = 37,092$	$N = 49,456$	$N = 61,816$
	SVM	Pearson	0.392	0.405	0.398	0.402	0.401	0.403
		$R^2$	0.151	0.163	0.158	0.161	0.161	0.162
		MAE	12.176	12.147	12.235	12.203	12.185	12.214
	RF	Pearson	0.335	0.347	0.344	0.353	0.359	0.359
		$R^2$	0.082	0.096	0.093	0.102	0.107	0.108
MAE		12.644	12.613	12.704	12.645	12.603	12.620	

387

388

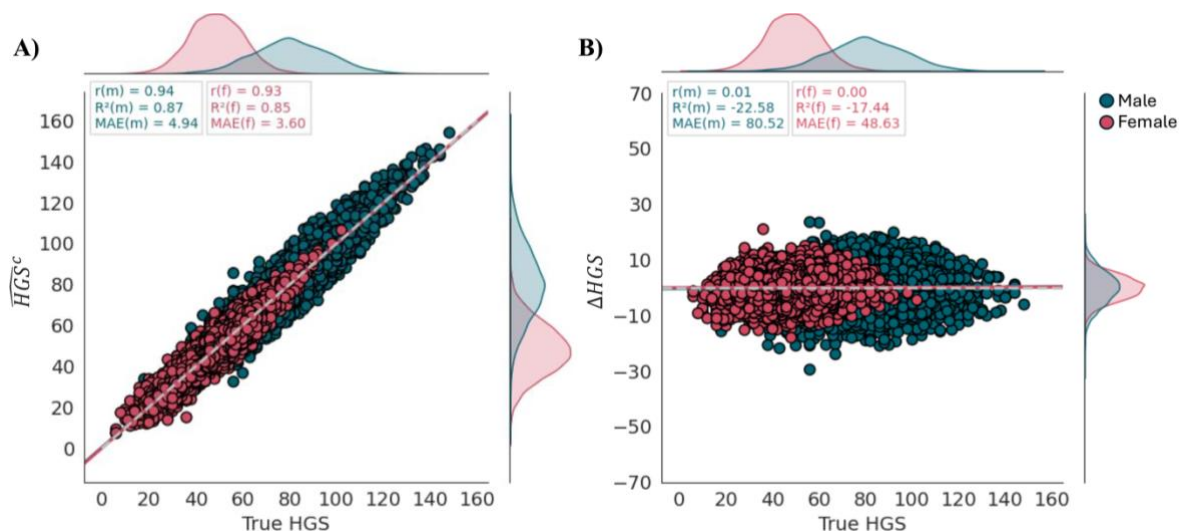
389

## Model Validation

390 To validate the selected linear SVM models, which were separately trained on the whole training dataset  
 391 for males and females. Then we applied them to the independent 10% HC test dataset, comprising 6,938  
 392 males and 8,969 females. After applying bias-correction to the predictions ( $\overline{HGS}^c$ ) on the test dataset,  
 393 prediction accuracy significantly improved compared to the uncorrected predictions (Additional file 1:  
 394 Figure S2). For males, the Pearson's correlation coefficients increased from  $r = 0.40$  (without bias-  
 395 correction) to  $r = 0.94$  (with bias-correction,  $p < 0.0001$ ), and for females, it improved from  $r = 0.42$   
 396 (without bias-correction) to  $r = 0.93$  (with bias-correction,  $p < 0.0001$ ), demonstrating enhanced  
 397 performance (Fig. 3A). The bias-correction was performed using the method proposed by Beheshti et

398 al. [40], involving the calculation of slope ( $\alpha$ ) and intercept ( $\beta$ ) by fitting a linear regression model  
 399 between true HGS and the residuals ( $\widehat{\Delta HGS} = \text{true HGS} - \widehat{HGS}$ ). Bias-correction parameters were  
 400 estimated separately for males ( $\alpha = 0.839$ ,  $\beta = -67.631$ ) and females ( $\alpha = 0.822$ ,  $\beta = -39.971$ ) using  
 401 predictions from out-of-sample validation sets generated via 10-fold CV on the HC training dataset. We  
 402 then assessed the models' unbiasedness by examining the correlation between  $\Delta HGS$  ( $\text{true HGS} -$   
 403  $\widehat{HGS}^c$ ) and true HGS (Fig. 3B). The analysis revealed no significant correlation between  $\Delta HGS$  and  
 404 true HGS for either males ( $r = 0.01$ ) or females ( $r = 0.00$ ), indicating an absence of bias in the corrected  
 405 predictions. Before bias-correction, correlations were  $r = 0.92$  for males and  $r = 0.91$  for females,  
 406 indicating some initial bias. This finding supports the conclusion that the model is unbiased across both  
 407 sexes.

408  
409



410

411 **Fig. 3** Relationship between  $\widehat{HGS}^c$  (A) and  $\Delta HGS$  (B) scores versus true HGS, respectively, after applying bias-correction method on the  
 412 independent non-brain-imaging HC test dataset, for males ( $N = 6,938$ ) and females ( $N = 8,969$ ). **A)** Scatter plot of  $\widehat{HGS}^c$  and true HGS:  
 413 for males ( $r = 0.94$ ,  $R^2 = 0.87$ ,  $MAE = 4.94$ ) and for females ( $r = 0.93$ ,  $R^2 = 0.85$ ,  $MAE = 3.6$ ). **B)** Scatter plot of  $\Delta HGS$  and true HGS: for  
 414 males ( $r = 0.01$ ,  $p = 0.41$ ) and for females ( $r = 0.00$ ,  $p = 0.73$ ). The dashed grey line in the A indicates the identity line ( $y = x$ ), while the  
 415 dashed grey line in the B indicates the reference line ( $y = 0$ ).

416

417 We then investigated the FI scores from the final models trained on the training dataset (90% of HC).  
 418 The models showed similarities and differences between males and females. Although the direction of  
 419 the contribution was the same for both sexes, the strength of contributing factors differed. For males,  
 420 the linear SVM model identified height and BMI as having positive contributions to HGS ( $FI_{\text{height}} = 4.94$  and  $FI_{\text{BMI}} = 3.00$ ), while WHR ( $FI_{\text{WHR}} = -2.57$ ) and age ( $FI_{\text{age}} = -2.83$ ) showed negative coefficients.  
 421 In females, height ( $FI_{\text{height}} = 3.27$ ) and BMI ( $FI_{\text{BMI}} = 0.67$ ) remained positive contributors, and WHR ( $FI_{\text{WHR}} = -0.53$ ) and age ( $FI_{\text{age}} = -3.07$ ) showed negative effects.  
 422  
423

424

### 425 **Reassessment reliability of $\Delta HGS$**

426 The reassessment reliability was evaluated using the concordance correlation coefficient (CCC)  
 427 between  $\Delta HGS$  values for two sessions: the baseline assessment visit as the initial session (session 0),  
 428 and the first repeat assessment visit (after 2-7 years) as reassessment (session 1) on the same participants  
 429 from the non-brain-imaging HC test dataset ( $N = 296$ , 54.73% female) without and with bias-correction.  
 430 The results demonstrated high reassessment reliability for  $\Delta HGS$  after applying bias-correction, with  
 431 males showing a CCC of 0.90 and females a CCC of 0.89. These values were notably higher compared  
 432 to the  $\Delta HGS$  without bias-correction (Table 5). The high reassessment reliability indicates that  $\Delta HGS$   
 433 scores remain stable despite physiological changes in participants' conditions over 2-7 years. This  
 434 reliability is crucial for application in the elderly population, where age and health-related changes

435 considerably affect HGS. The strong agreement between sessions, shown by high CCC values, confirms  
436 the reliability of the sex-specific models.

437

438 **Table 5** CCC between baseline and follow-up delta values, and MAE with and without bias correction

Sex	N	Without bias-correction			With bias-correction		
		MAE (Session 0)	MAE (Session 1)	CCC	MAE (Session 0)	MAE (Session 1)	CCC
Female	162	8.129	12.059	0.32	3.294	3.496	0.89
Male	134	12.934	16.434	0.47	4.534	4.475	0.90

439

440

### 441 **Association between HGS scores and brain structure**

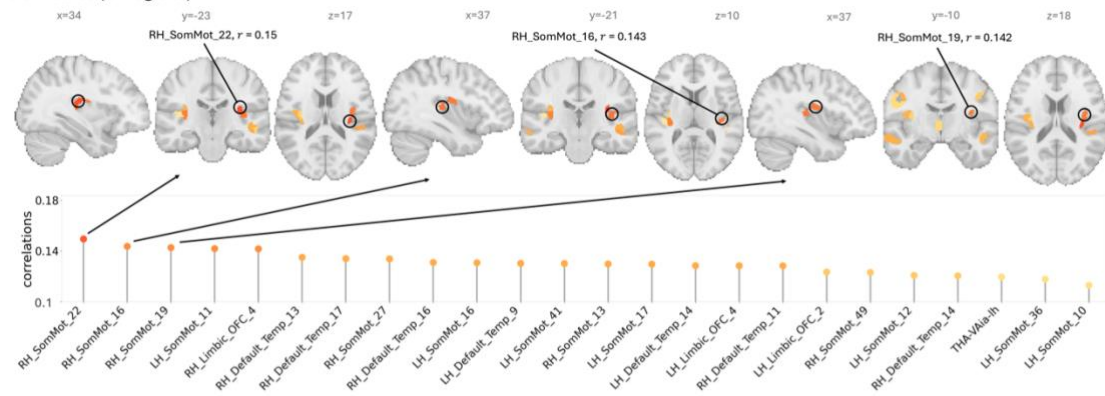
442 We investigated Pearson’s  $r$  between regional GMV and two HGS scores, true HGS and  $\Delta HGS$  in a  
443 large cohort of HC (7,726 males and 9,292 females). Each participant’s data included 1,088 regional  
444 GMV features covering the whole brain (see the “Imaging data and preprocessing” section). Significant  
445 correlations were identified for both true HGS and  $\Delta HGS$  after applying Bonferroni correction  
446 ( $p_{\text{corrected}} < 0.05$ ). Fig. 4 demonstrates the distribution of associations between regional GMV and  
447 HGS. The cortical region labeling was derived from the Schaefer 1000-parcel 7-network brain atlas.

448 For true HGS, significant correlations were found in 878 regions for males and 660 for females. All  
449 correlations were positive. When applying a correlation threshold of  $|r| > 0.1$ , 364 regions remained in  
450 males and 24 in females. The intersection of significant regions between sexes included 24 regions,  
451 none of which were located in cerebellar areas. These results indicate a broader association between  
452 true HGS and GMV in males compared to females, suggesting potential sex differences. The average  
453 correlations between true HGS and regional GMV of the intersecting significant regions for both sexes  
454 showed values ranging from 0.113 to 0.15 (Fig. 4A). The strongest correlations were observed in the  
455 cortical right hemisphere somatomotor regions, parcels 22 (RH\_SomMot\_22,  $r = 0.15$ ), 16  
456 (RH\_SomMot\_16,  $r = 0.143$ ), and 19 (RH\_SomMot\_19,  $r = 0.142$ ). Subcortical associations differed  
457 across sexes (Additional file 1: Table S3), with the highest subcortical association found in the left  
458 hemisphere inferior ventral anterior division of the thalamus (THA-VAia-lh,  $r = 0.12$ ). The results  
459 showed that a higher HGS is linked with increased GMV in the cortical areas, which are crucial for  
460 motor control.

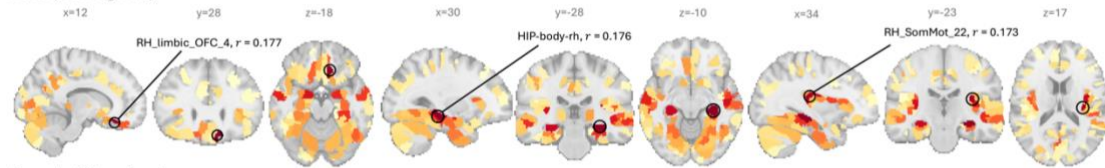
461 In contrast,  $\Delta HGS$  demonstrated significant correlations in 968 regions for males and 993 regions for  
462 females. After applying the threshold of  $|r| > 0.1$ , 698 regions in males and 755 regions in females  
463 remained. The intersection of significant regions between sexes retained 667 regions, highlighting the  
464 consistency and robustness of the association between the  $\Delta HGS$  score and GMV. The average  
465 correlations for these intersecting significant regions ranged from -0.298 to -0.101 (Fig. 4B). The only  
466 positive correlations were observed in females within subcortical regions, specifically in the anterior  
467 globus pallidus of the left hemisphere (aGP\_lh,  $r = 0.157$ ) and the right hemisphere (aGP\_rh,  $r = 0.145$ ).  
468 For both sexes, the strong associations included the right hemisphere somatomotor cortical region from  
469 the somatosensory network, parcel 19 (RH\_SomMot\_19,  $r = -0.298$ ), followed by parcel 22  
470 (RH\_SomMot\_22,  $r = -0.291$ ), and parcel 16 (RH\_SomMot\_16,  $r = -0.275$ ). This pattern persisted in  
471 sex-specific analyses, with males showing strong correlations in RH\_SomMot\_19 ( $r = -0.28$ ) and  
472 RH\_SomMot\_22 ( $r = -0.274$ ), while females demonstrated even stronger correlations in these regions  
473 (RH\_SomMot\_19:  $r = -0.315$ ; RH\_SomMot\_22:  $r = -0.307$ ). Subcortical associations differed across  
474 sexes (Additional file 1: Table S4), with the highest subcortical association in both sexes was found in  
475 the left hemisphere hippocampal body (HIP-body-lh,  $r = -0.235$ ). The most significant cerebellar  
476 association was observed in the left lobule VI (Left\_VI) for both sexes ( $r = -0.214$ ). The higher number  
477 of significant and stronger correlations observed across a broader range of brain areas suggest that  
478  $\Delta HGS$  can be a more sensitive score for detecting brain structure relationships. Furthermore, the  
479 significant increase in overlapping regions suggested a common neurobiological basis beyond sex  
480 differences.

**A) True HGS and regional GMV associations**

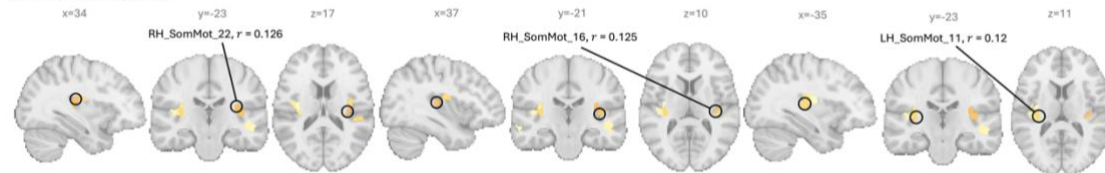
Both sexes (24 regions)



Male (364 regions)

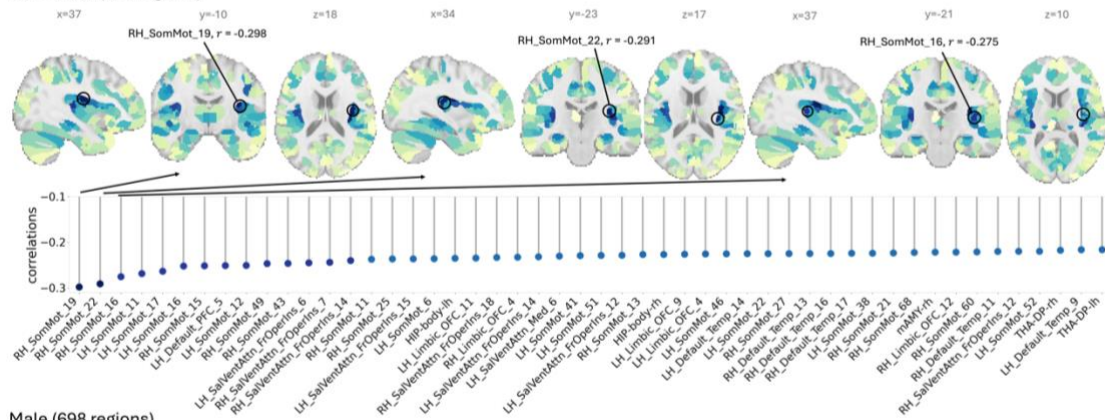


Female (24 regions)

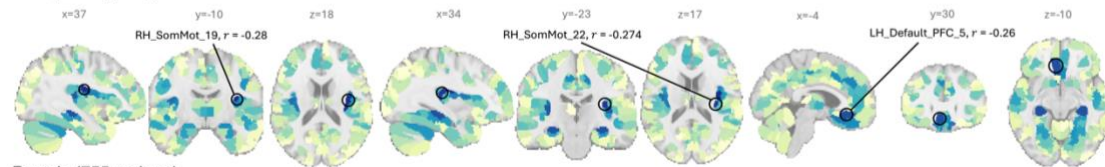


**B) ΔHGS and regional GMV associations**

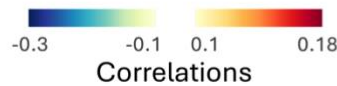
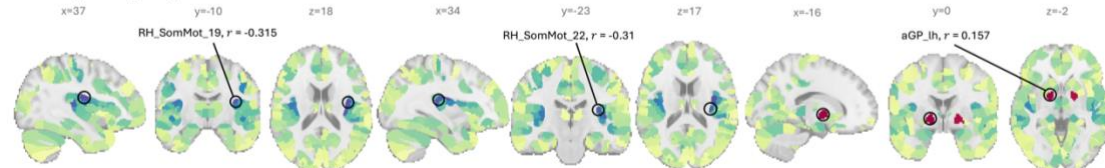
Both sexes (667 regions)



Male (698 regions)



Female (755 regions)



481  
482  
483

**Fig. 4** Regional distribution of associations between GMV and HGS, after applying Bonferroni correction ( $p_{corrected} < 0.05$ ) and focusing on significant regions with  $|r| > 0.1$ . **A) True HGS and GMV correlation:** Both sexes (24 regions): The average correlation

484 between intersecting of significant regions in both sexes ranged ( $0.113 \leq r \leq 0.15$ ). The strongest cortical correlation ( $r = 0.15$ ) was  
485 observed in “RH\_SomMot\_22”, the strongest subcortical correlation ( $r = 0.12$ ) in “THA-VAia-lh”. No cerebellar regions were identified  
486 among these 24 regions. The scatter plot represents the correlation of these 24 significant regions. Males (364 regions): Correlations  
487 ranged ( $0.1 \leq r \leq 0.177$ ), with the strongest cortical correlation ( $r = 0.177$ ) in “RH\_Limbic\_OFC\_4”, the strongest subcortical correlation  
488 ( $r = 0.176$ ) in “HIP-body-rh”, and the highest cerebellar correlation ( $r = 0.133$ ) in “Left\_VI”. Females (24 regions): Correlations ranged  
489 ( $0.1 \leq r \leq 0.126$ ), with the strongest cortical correlation ( $r = 0.126$ ) in “RH\_SomMot\_22”, the strongest subcortical correlation ( $r = 0.113$ )  
490 in “THA-VAia-lh”, and no cerebellar regions were significant. **B)  $\Delta HGS$  and GMV correlation:** Both sexes (667 regions): The average  
491 correlations between the intersecting of significant regions in both sexes ranged ( $-0.298 \leq r \leq -0.101$ ), with the strongest cortical  
492 correlation ( $r = -0.298$ ) in “RH\_SomMot\_19”, the strongest subcortical correlation ( $r = -0.235$ ) in “HIP-body-lh”, and the highest  
493 cerebellar correlation ( $r = -0.214$ ) in “Left\_VI”. The scatter plot represents the 50 top significant regions. Males (698 regions): Correlations  
494 ranged ( $-0.28 \leq r \leq -0.1$ ), with the strongest cortical correlation ( $r = -0.28$ ) in “RH\_SomMot\_19”, the highest subcortical association ( $r =$   
495  $-0.256$ ) in the “HIP-body-rh”, and the highest cerebellar correlation ( $r = -0.222$ ) in the “Left\_VI”. Females (755 regions): Correlations  
496 ranged ( $-0.315 \leq r \leq 0.157$ ), with the strongest cortical correlation ( $r = -0.315$ ) in “RH\_somMot\_19”, the strongest subcortical correlation  
497 ( $r = -0.231$ ) in “THA-DP-rh”, the highest cerebellar correlation ( $r = -0.205$ ) in “Left\_VI”. Two subcortical regions, “aGP\_lh” ( $r = 0.157$ )  
498 and “aGP\_rh” ( $r = 0.145$ ), showed positive correlations.

499

500

### 501 **Evaluation of pre-to-post disease longitudinal HGS changes**

502 The innovative aspect of this study is the implementation of a longitudinal design, which captures HGS  
503 scores at two critical time points: before (pre) and after (post) disease onset. Capturing longitudinal  
504 changes in HGS can improve our understanding of the dynamic relationship between HGS and disease  
505 onset and progression, providing valuable insights into how disease impacts physical function over time.  
506 Such changes can provide insights into an individual’s health status, the effectiveness of training or  
507 rehabilitation programs, and the progression of various health conditions. To analyze this longitudinal  
508 data, we employed a two-way ANOVA, separately for each sex. The analyses included group  
509 (patient/control) as the between-subject factor and time-point (pre/post) as the within-subject factor,  
510 with either true HGS or  $\Delta HGS$  as the dependent scores. We analyzed the stroke and MDD cohorts  
511 separately with 10 matched HC for each patient (Table 3).

512 A significant main effect of time-point was observed for both patient cohorts, indicating time-  
513 dependent changes in HGS and  $\Delta HGS$  across patients and healthy controls (Table 6). In stroke patients,  
514 a significant interaction was observed in males for both true HGS ( $F_{1,438} = 4.434$ ,  $p = 0.036$ ) and  $\Delta HGS$   
515 ( $F_{1,438} = 9.91$ ,  $p = 0.002$ ). Post-hoc analysis revealed the significant differences in matched HC between  
516 pre and post time-points for both scores ( $p < 0.0000$ ), and in patients between pre and post time-points  
517 for  $\Delta HGS$  score ( $p = 0.0332$ ). No significant group differences were found at any time point, and no  
518 significant interactions were observed in female stroke patients (Fig. 5).

519 In MDD patients, significant interactions were observed in both females and males for  $\Delta HGS$  (males:  
520  $F_{1,405} = 5.404$ ,  $p = 0.021$ ; females:  $F_{1,658} = 8.844$ ,  $p = 0.003$ ) and true HGS (males:  $F_{1,405} = 4.362$ ,  $p =$   
521  $0.037$ ; females:  $F_{1,658} = 9.928$ ,  $p = 0.002$ ). Post-hoc analysis showed significant differences between  
522 pre and post time-points in matched HC for both scores and sexes (all  $p < 0.0000$ ) as well as in female  
523 patients for the  $\Delta HGS$  score only ( $p = 0.0005$ ). No significant group differences were observed at any  
524 time point. (Fig. 5).

525 The interaction plots provide valuable insights into the trajectory of true HGS and  $\Delta HGS$  among patients  
526 with stroke and MDD in comparison to matched HC for both males and females from pre to post time-  
527 points (Fig. 5). For both sexes, true HGS showed a less strong decline from pre to post time-points in  
528 patients compared to their matched HC groups.  $\Delta HGS$ , in contrast, demonstrated a significant increase  
529 from pre- to post- time-points in all groups, indicating an improvement in HGS relative to the expected  
530 HGS predicted based on anthropometrics and age. This increase seems to be stronger in patients  
531 compared to controls.

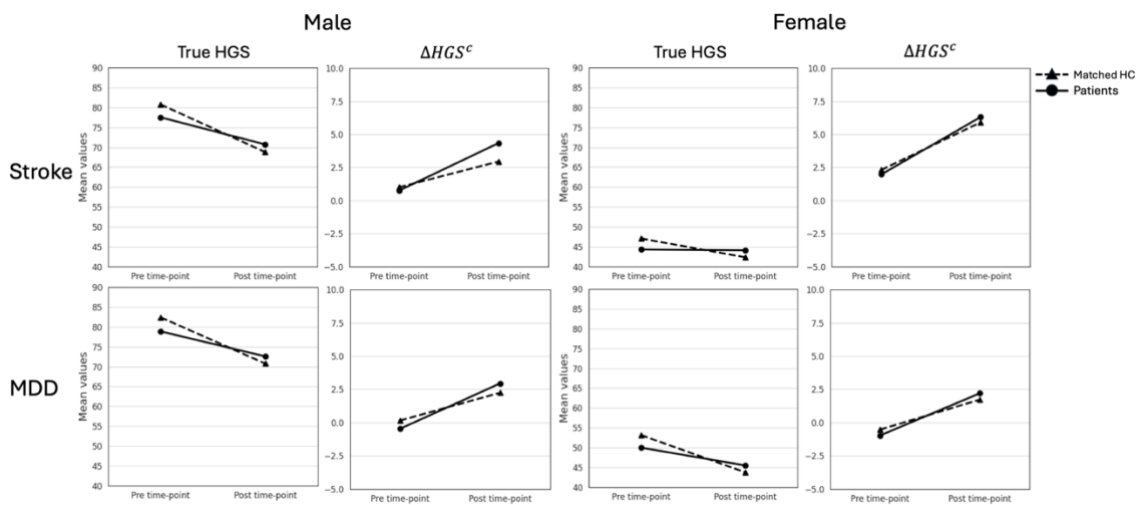
532 To assess whether the change between pre and post time-points differed significantly between groups,  
533 we calculated the difference scores for both true HGS and  $\Delta HGS$  by subtracting the pre time-point  
534 values from the post time-point values for each group, separately for males and females. Independent t-  
535 tests were then conducted to compare these difference scores between patients and matched HC groups.  
536 This approach allows for a direct comparison of the magnitude and direction of change across groups.

537 In stroke, significant differences were observed only in males who exhibited smaller declines in true  
 538 HGS compared to matched HC (stroke: -6.80 kg vs matched HC: -11.95 kg,  $p = 0.035$ ) and larger  
 539 increases in  $\Delta HGS$  (stroke: 3.59 kg vs matched HC: 1.94 kg,  $p = 0.001$ ). MDD patients of both sexes  
 540 showed significant differences. For true HGS, patients demonstrated smaller decline than matched HC  
 541 (males: MDD: -6.30 kg vs matched HC: -11.66 kg,  $p = 0.037$ ; females: MDD: -4.50 kg vs matched HC:  
 542 -9.43 kg,  $p = 0.002$ ). Conversely, for  $\Delta HGS$ , patients exhibited greater increases (males: 3.41 kg vs 2.09  
 543 kg,  $p = 0.02$ ; females: 3.17 kg vs 2.26 kg,  $p = 0.003$ ).

544  
 545 **Table 6** Sex-specific ANOVA and post-hoc results for Group (matched HC vs. patient) and Time-point (pre, post)

Disease	Sex	Source	True HGS		$\Delta HGS$		
			<i>F</i>	<i>p</i>	<i>F</i>	<i>p</i>	
Stroke	Female	Group	0.036	0.85	0.001	0.977	
		Patients ( <i>N</i> = 16)	25.086	0.000	376.401	0.000	
		Matched HC ( <i>N</i> = 160)	<b>Interaction (Group:Time-point)</b>				
	Male	Group	0.078	0.78	0.365	0.546	
		Patients ( <i>N</i> = 40)	266.505	0.000	193.944	0.000	
		Matched HC ( <i>N</i> = 400)	<b>Interaction (Group:Time-point)</b>				
	<b>Post-Hoc Test:</b>			<b>meandiff</b>	<b>p</b>	<b>meandiff</b>	<b>p</b>
	patients post time-point vs matched HC post time-point			1.9125	0.8904	1.3916	0.4841
	patients pre time-point vs matched HC pre time-point			-3.24	0.6177	-0.2537	0.9939
	patient pre time-point vs patient post time-point			6.8	0.2328	-3.5882	<b>0.0332</b>
matched HC pre time-point vs matched HC post time-point			11.9525	<b>0.0000</b>	-1.9429	<b>0.0000</b>	
MDD	Female	Group	0.266	0.606	0.001	0.976	
		Patients ( <i>N</i> = 60)	398.997	0.000	696.981	0.000	
		Matched HC ( <i>N</i> = 600)	<b>Interaction (Group:Time-point)</b>				
	Male	Group	0.117	0.732	0.001	0.969	
		Patients ( <i>N</i> = 37)	228.97	0.000	182.535	0.000	
		Matched HC ( <i>N</i> = 370)	<b>Interaction (Group:Time-point)</b>				
	<b>Post-Hoc Test:</b>			<b>meandiff</b>	<b>p</b>	<b>meandiff</b>	<b>p</b>
	patients post time-point vs matched HC post time-point			1.7517	0.6865	0.4755	0.8571
	patients pre time-point vs matched HC pre time-point			-3.175	0.1873	-0.4411	0.8822
	patient pre time-point vs patient post time-point			4.5	0.1519	-3.1726	<b>0.0005</b>
matched HC pre time-point vs matched HC post time-point			9.4267	<b>0.0000</b>	-2.256	<b>0.0000</b>	
<b>Post-Hoc Test:</b>			<b>meandiff</b>	<b>p</b>	<b>meandiff</b>	<b>p</b>	
patients post time-point vs matched HC post time-point			1.8216	0.9171	0.7005	0.9077	
patients pre time-point vs matched HC pre time-point			-3.5432	0.5916	-0.6229	0.9329	
patient pre time-point vs patient post time-point			6.2973	0.3485	-3.4141	0.0727	
matched HC pre time-point vs matched HC post time-point			11.6622	<b>0.0000</b>	-2.0907	<b>0.0000</b>	

546



547

548 **Fig. 5** Changes in HGS among patients with stroke and MDD compared to matched HC across two time-points: pre and post time-points.  
 549 The dashed lines represent the matched control group, while the solid lines depict the patient groups. These findings underscore the  
 550 importance of considering both absolute and relative scores of muscle strength in understanding the physical capabilities of individuals  
 551 with neurological and psychiatric diseases. The increased  $\Delta HGS$  suggests that despite the decline in true HGS, patients and matched HC  
 552 may perform better than expected when accounting for baseline physical attributes.

## Discussion

In this study, we explored whether HGS can be predicted based on anthropometric and demographic measurements and sought to uncover biological insights by analyzing the predicted HGS values. We developed a new individual-level score  $\Delta HGS$  that captures how HGS deviates from the expected value based on an individual's characteristics. To this end, we used data from the UK Biobank.

First, we performed ML analysis to predict combined HGS using anthropometric factors (i.e., BMI, height, and WHR) and demographic parameters age and sex. The use of combined HGS, the sum of the grip strengths of both hands, as the target was particularly used as a comprehensive measure of overall strength [33], mitigating the potential biases introduced by handedness or unilateral strength differences [34]. We developed sex-specific models to account for known differences in HGS between males and females, specifically HGS values are consistently higher in males compared to females across all age ranges [15,22–24]. We employed linear SVM and RF regression models for HGS prediction across different sample sizes within a CV scheme. The inclusion of a nonlinear model (RF) alongside the linear SVM was based on the documented nonlinear relationship between age and HGS (Chandrasekaran et al. [20]). In our analysis, linear SVM outperformed RF in predicting combined HGS, achieving higher performance for both sexes. The prediction accuracy improved with larger sample sizes, but smaller samples exhibited higher variance, highlighting the significance of using enough data to adequately capture the variability in demographic and anthropometric factors and their relationship with HGS (Fig. 2, Table 4).

The linear SVM model identified that height and BMI positively contributed to HGS prediction in both sexes, while WHR and age contributed negatively. The magnitude of contributions differed by sex: height and BMI showed a stronger positive contribution in males compared to females (males:  $FI_{\text{height}} = 4.94$ ,  $FI_{\text{BMI}} = 3.00$ ; females:  $FI_{\text{height}} = 3.27$ ,  $FI_{\text{BMI}} = 0.67$ ). WHR had lower contributions in females than males (males:  $FI_{\text{WHR}} = -2.57$ ; females:  $FI_{\text{WHR}} = -0.53$ ). Age contributed negatively for both sexes, reflecting the expected decline of HGS with age (males:  $-2.83$ ; females:  $-3.07$ ). These findings align with known associations between these variables and HGS (see the “Model Validation” section). The varying feature importance between sexes taken together with the higher prediction accuracy for males highlight the complex interplay of anthropometric and demographic factors and their association with HGS. The differential contribution of weight-related factors to HGS in females compared to males may be due to sex-specific differences in body composition. Females generally have higher body fat and lower muscle mass than males which could explain why weight-related variables are less predictive of HGS in females [55]. Additionally, hormonal factors, particularly estrogen levels, play a significant role in muscle strength and function in females, potentially overshadowing the influence of weight-related variables on HGS [56].

Our results are in line with the well-established positive relationship between HGS and both BMI and height across various populations and age groups (e.g., M. A. Agtuahene et al. [19] and Yong-Hao Pua et al. [17]). B. Bhattacharjee et al. [18] have reported an inverse relationship between HGS and WHR, which reflects the proportion of abdominal fat relative to hip circumference. Age shows variations in HGS across different age groups. HGS generally declines with age, but the relationship is complex and influenced by sex [16,21]. HGS typically increases during childhood and adolescence, peaks in early adulthood, and then declines with age, particularly after 40 [16]. Vianna et al. [21] found that the onset of HGS decline differs between sexes, beginning earlier in men (around age 30) compared to women (around age 50). The aging process results in progressive muscle loss, impacting HGS. De Araújo et al. [16], identified various factors associated with low HGS in older adults, including age-related differences, emphasizing the multifaceted nature of HGS decline across the lifespan. Given this nonlinear relationship between age and HGS, it is intriguing to consider that our result showed the linear SVM model to be more accurate than the nonlinear RF model. This may be explained by the high mean age in the UKB data. De Araújo et al. [16] also revealed that factors such as socioeconomic status, physical activity levels, and chronic health conditions can influence HGS in older populations, indicating that HGS is also determined by environmental and lifestyle factors. A previous ML study



603 also demonstrated a high prediction accuracy using posture, anthropometric, and demographic variables  
604 [57]. This suggests that adding further variables with more detailed body measurements, environmental  
605 and lifestyle can help in increasing accuracy. However, large datasets with those variables are currently  
606 not available.

607 The predictions obtained by our models exhibited a bias (Additional file 1: Figure S2), with residuals  
608 correlating with the target. To address this, we applied a bias-correction method [40], resulting in bias-  
609 free predictions resulting in enhanced accuracy (Fig. 3). The difference between the true HGS and bias-  
610 free predicted HGS ( $\Delta HGS = true\ HGS - \overline{HGS}^c$ ) was then calculated as a novel score which was then  
611 used for further analysis together with the measured or true HGS.

612 We explored the neurobiological underpinnings of muscular strength by analyzing the relationship  
613 between GMV and two HGS scores. We found that higher HGS is associated with higher GMV in key  
614 brain regions involved in motor but also regions playing a role in other functions (Fig. 4). These findings  
615 suggest that HGS as a measure of physical capability is reflected in structural brain integrity. However,  
616 it is crucial to consider potential confounding effects in these associations, particularly the influence of  
617 age. Age has a strong effect on both HGS and GMV and as individuals age, both muscle strength and  
618 brain volume typically decrease. Other potential confounders, such as physical activity levels, body  
619 composition (e.g., muscle mass, body fat percentage), nutritional status, hormonal factors, genetic  
620 predisposition, and socioeconomic status, should also be considered. These factors may independently  
621 influence both HGS and GMV, potentially complicating the interpretation of their relationship. Existing  
622 literature has shown that HGS is linked to brain structures in frontal, temporal, subcortical, and  
623 cerebellar regions. Our findings also revealed associations between HGS and these areas. For instance,  
624 Jiang et al. [1] reported widespread positive associations, especially in subcortical regions and temporal  
625 cortices, even after controlling for various confounders including age, sex, education level,  
626 socioeconomic status, BMI, height, and WHR. Similarly, Meysami et al. [58] reported that greater HGS  
627 is associated with larger hippocampal volume, and also stronger dominant HGS was related to larger  
628 frontal lobe volumes in older adults. In our results, we found that the hippocampal as well as thalamus  
629 regions were associated with HGS in both males and females, along with specific associations in the  
630 frontal regions (see Additional file 1: Table S3).

631 The  $\Delta HGS$  score demonstrated stronger and more widely distributed correlations with GMV compared  
632 to true HGS, particularly in motor-related brain regions (Fig. 4). These correlations were significant  
633 across various cortical, subcortical, and cerebellar brain regions in both males and females (Fig. 4). The  
634 intersection of significant regions between the sexes revealed 667 regions (only 24 for true HGS), while  
635 698 and 755 significant regions were identified in males and females, respectively. Overall, our results  
636 suggest that  $\Delta HGS$  is better at capturing the neurobiological basis of muscular strength in both sexes  
637 compared to true HGS, suggesting that  $\Delta HGS$  may reflect unique aspects of brain structure beyond what  
638 true HGS alone reveals. In contrast to the GMV-true HGS relationships which were all positive, the  
639 associations to  $\Delta HGS$  were all negative. The negative GMV- $\Delta HGS$  correlations suggest that individuals  
640 with lower true HGS compared to their predicted HGS tend to have larger GMV. This suggests better  
641 preserved brain volume despite lower strength than expected. This relationship becomes more intriguing  
642 when considering factors influencing the difference in HGS. Negative  $\Delta HGS$  values might signal an  
643 accelerated decline in strength, in which the person is experiencing a more rapid loss of strength than  
644 expected for their age or possibly reflecting age-related health concerns that disproportionately affect  
645 muscle strength, as muscle strength is a reliable indicator of overall health status in aging populations  
646 [7]. Speculatively, a high negative  $\Delta HGS$  could suggest unfavorable body composition or sarcopenic  
647 obesity, a condition where muscle loss is combined with excess fat [59].

648 We then investigated whether changes over time in true HGS and  $\Delta HGS$  differed between patients  
649 with either stroke or MDD and their corresponding matched HC in a longitudinal design. We observed  
650 a significant reduction in change HGS scores (difference between pre and post disease onset) in both  
651 stroke and MDD patients compared to their corresponding matched HC (Table 3), with HC showing a  
652 significant decrease in HGS but patients no or less change. Among stroke patients, the decrease in HGS

653 is likely to happen due to damage of the upper motor neuron in the precentral gyrus or of its descending  
654 output, i.e., the corticospinal tract, leading to motor impairment, especially of the contralateral hand.  
655 Stroke patients typically have lower HGS compared to HC, especially in the early stages post-stroke  
656 [60]. ANOVA results revealed sex-specific patterns, with male stroke patients showing significant  
657 interactions in both true HGS ( $p = 0.036$ ) and  $\Delta HGS$  ( $p = 0.002$ ), while no significant interactions were  
658 observed in female stroke patients. These sex differences align with previous research suggesting  
659 different recovery patterns between males and females post-stroke [61]. Importantly, this cannot be  
660 because of differing recovery times as the time between disease onset and post assessment was not  
661 significantly different between males and females ( $p = 0.59$ ).

662 Interestingly, despite these longitudinal differences, both HGS and  $\Delta HGS$  were not effective in  
663 differentiating between patients and matched HC at the post time-point. This lack of distinction may be  
664 attributed to several factors, including the limited number of stroke patients with motor area lesions,  
665 potentially masking the effects of these impairments on HGS scores. Importantly, ischemic lesions  
666 outside key motor regions or the corticospinal tract do not usually lead to reductions in grip force. In  
667 our cohort of 56 stroke patients (1 female patient hemorrhagic), identified using ICD-10 codes without  
668 including self-reported cases, post-stroke neuroimaging data were available for 25 patients (44.64%).  
669 Among these, 14 patients (56%) presented lesions in motor-related regions, with 9 of them exhibiting  
670 lesions affecting the contralateral hand. Additional factors include the substantial time elapsed between  
671 pre and post assessments in both disease cohorts which may reflect the effects of treatment and  
672 rehabilitation efforts over time. Specifically, in stroke patients, the average interval between pre and  
673 post assessments was approximately 9.26 years for males and 9.5 years for females, with post-stroke  
674 assessments occurring between 0.18-11.14 years for males and 0.04-9.78 years for females after stroke  
675 onset.

676 In MDD patients, the reduction in HGS may be due to the multifactorial impact of MDD on physical  
677 health [62], which is attributed to the complex interplay between depression and physical health.  
678 Ganipineni et al. [10] found that individuals with depressive symptoms tend to have lower HGS  
679 compared to those without. Trivedi [62] showed that MDD not only affects mental health but also has  
680 wide-ranging effects on physical health through various mechanisms. These include decreased physical  
681 activity, changes in appetite and nutrition, sleep disturbances, hormonal and inflammatory alterations,  
682 and potential medication side effects, all of which can contribute to reduced grip strength. ANOVA  
683 results showed significant interactions in true HGS (males:  $p = 0.037$ ; females:  $p = 0.002$ ) and  $\Delta HGS$   
684 (males:  $p = 0.021$ ; females:  $p = 0.003$ ) for both sexes, in contrast to the sex-specific patterns observed  
685 in stroke patients. However, despite these longitudinal differences, both HGS and  $\Delta HGS$  were  
686 ineffective in distinguishing MDD patients from matched HC at the post time-point. This finding may  
687 reflect the prolonged time elapsed between pre and post assessments, with the mean time intervals of  
688 9.46 years for males and 9.3 years for females. Post-MDD assessments occurred within 0.02-9.63 years  
689 for males and 0.02-11.98 years for females, highlighting the influence of ongoing treatment and  
690 rehabilitation. Further research could provide deeper insights into the relationship between muscle  
691 function and diseases, supporting early detection, targeted prevention, and monitoring of disease  
692 progression in neurological and psychiatric conditions.

693 Our study faced several limitations that should be addressed in future research. Firstly, the  
694 demographic (age and sex) and anthropometric variables (BMI, height, and WHR) may not capture all  
695 relevant factors influencing muscle strength, potentially overlooking other predictors like more detailed  
696 body measurements, genetics, and lifestyle factors. Secondly, the study sample was drawn from the  
697 UKB, which may not be representative of other populations, potentially limiting the generalizability of  
698 the findings to more diverse demographic groups. Thirdly, the study used a limited number of ML  
699 models, focusing on linear SVM and RF, which may not fully capture the complexity of the data.  
700 Although we covered linear and non-linear models, exploring other models could potentially improve  
701 prediction accuracy. Lastly, the longitudinal study was constrained by small sample sizes for stroke and  
702 MDD patients, which could affect the statistical power and reliability of the results. Here, we relied on

703 incidental data from the UKB, which comes with limitations such as low sample sizes, the small number  
704 of stroke patients with motor area related lesions, and lack of detailed information regarding medication  
705 and rehabilitation.

706  
707

## 708 Conclusion

709 This study demonstrates that HGS can be predicted using demographic and anthropometric variables at  
710 moderate accuracy through machine learning models, particularly linear SVM. The novel  $\Delta HGS$  score,  
711 representing the difference between true and bias-free predicted HGS, showed stronger and widely  
712 distributed correlations with GMV compared to true HGS, especially in motor-related brain regions.  
713 This suggests  $\Delta HGS$  maybe a more sensitive biomarker for brain health assessment. Both true HGS and  
714  $\Delta HGS$  did not capture longitudinal differences between patients and matched HC. Further research is  
715 needed to validate these results in more diverse populations and explore the mechanisms linking HGS  
716 changes to specific diseases. Overall, this study provides a foundation for enhancing the utility of HGS  
717 as a biomarker in neurological and psychiatric research and clinical practice.

718  
719

## 720 Abbreviations

HGS	Handgrip strength
HC	Healthy controls
MDD	Major depressive disorder
GMV	Grey matter volume
ML	Machine learning
SVM	Support Vector Machine
RF	Random Forest
FI	Feature importance
MAE	Mean absolute error
CCC	Concordance correlation coefficient

721  
722

## 723 Supplementary Information

724 The online version contains supplementary material available at the additional supplementary file  
725 (supplementary.pdf)

726  
727

**Additional file 1: Table S1.** Summary of the characteristics of the HC participants for matched sample analysis.  
728 **Table S2.** Summary of the characteristics of the non-imaging HC participants on test dataset for reassessment reliability  
729 analysis. **Table S3.** Summary of the top 10 subcortical regions with strongest correlation with true HGS. **Table S4.**  
730 Summary of the top 10 subcortical regions with strongest correlation with  $\Delta HGS$ . **Figure S1.** Flowchart of UKB  
731 participants selection and included in the analysis. **Figure S2.** Scatter plots depicting the relationship between various  
732 scores of  $\overline{HGS}$  and  $\overline{\Delta HGS}$  without bias-correction versus true HGS on the independent non-brain-imaging HC test dataset,  
733 for males and females.

734  
735

## 736 Acknowledgments

737 This research has been conducted using data from UK Biobank resources (application number 41655). All data used in this  
738 study are publicly accessible from UK Biobank via their standard data access procedure (<http://www.ukbiobank.ac.uk/>).

739  
740

## 740 Authors' contributions

741 All authors read and approved the final manuscript. We use the CRediT contributor role taxonomy to describe individual  
742 contributions to the paper. Conceptualization: K.N., S.B.E., C.G., K.R.P., L.H., V.M.; Data curation: K.N., C.T., V.K., K.R.P.;  
743 Formal analysis: K.N.; Methodology: K.N., S.B.E., L.H., V.M., C.G., K.R.P.; Supervision: C.G., S.B.E., K.R.P.;

744 Visualization: K.N., Writing—original draft: K.N.; Writing—review & editing: K.N., S.B.E, G. A, L.H., C.T., V.K, F.R.,  
745 V.M., C.G., K.R.P.

746

## 747 **Funding**

748 This research was funded by the Deutsche Forschungsgemeinschaft (DFG, German Research Foundation) - Project-ID  
749 431549029 - Collaborative Research Centre CRC1451 on motor performance project B05.

750

## 751 **Availability of data**

752 All data used in this study are publicly available through the UK Biobank, accessible via their standard data access procedure  
753 at <http://www.ukbiobank.ac.uk/>.

754

## 755 **Declarations**

756

### 757 **Ethics approval and consent to participate**

758 The UK Biobank study was approved by the North West Multicenter Research Ethics Committee (No. 16/NW/0274), with  
759 written informed consent obtained from all participants. A re-analysis of the anonymized data was approved by the ethics  
760 committee of the Heinrich Heine University Düsseldorf (2018-317-RetroDEuA).

761

### 762 **Consent for publication**

763 Not applicable.

764

### 765 **Competing interests**

766 The authors declare no competing interests.

767

## 768 **Author details**

769 <sup>1</sup> Department of Neurology, Faculty of Medicine and University Hospital Cologne, University of Cologne, Cologne, Germany. <sup>2</sup> Institute of Neuroscience  
770 and Medicine, Brain & Behaviour (INM-7), Research Centre Jülich, Jülich, Germany. <sup>3</sup> Institute of Neuroscience and Medicine, Cognitive Neuroscience  
771 (INM-3), Research Centre Jülich, Jülich, Germany <sup>4</sup> Institute of Systems Neuroscience, Medical Faculty and University Hospital Düsseldorf, Heinrich  
772 Heine University, Düsseldorf, Germany. <sup>5</sup> Goethe University Frankfurt, Department of Neurology, Frankfurt University Hospital, Frankfurt am Main,  
773 Germany. <sup>6</sup> Department of Biology, Faculty of Mathematics and Natural Sciences, Heinrich Heine University Düsseldorf, Düsseldorf, Germany.

774 \* Correspondence to Kimia Nazarzadeh ([kimia.nazarzadeh@uk-koeln.de](mailto:kimia.nazarzadeh@uk-koeln.de)) and Kaustubh R. Patil ([k.patil@fz-juelich.de](mailto:k.patil@fz-juelich.de))

775

776

777

## 778 **Reference**

- 779 [1] Jiang R, Westwater ML, Noble S, Rosenblatt M, Dai W, Qi S, et al. Associations between grip  
780 strength, brain structure, and mental health in > 40,000 participants from the UK Biobank. *BMC  
781 Medicine* 2022;20:286. <https://doi.org/10.1186/s12916-022-02490-2>.
- 782 [2] Roberts HC, Denison HJ, Martin HJ, Patel HP, Syddall H, Cooper C, et al. A review of the  
783 measurement of grip strength in clinical and epidemiological studies: towards a standardised  
784 approach. *Age and Ageing* 2011;40:423–9. <https://doi.org/10.1093/ageing/afr051>.
- 785 [3] Duchowny KA, Ackley SF, Brenowitz WD, Wang J, Zimmerman SC, Caunca MR, et al.  
786 Associations Between Handgrip Strength and Dementia Risk, Cognition, and Neuroimaging  
787 Outcomes in the UK Biobank Cohort Study. *JAMA Netw Open* 2022;5:e2218314.  
<https://doi.org/10.1001/jamanetworkopen.2022.18314>.
- 788 [4] Celis-Morales CA, Petermann F, Hui L, Lyall DM, Iliodromiti S, McLaren J, et al. Associations  
789 Between Diabetes and Both Cardiovascular Disease and All-Cause Mortality Are Modified by  
790 Grip Strength: Evidence From UK Biobank, a Prospective Population-Based Cohort Study.  
791 *Diabetes Care* 2017;40:1710–8. <https://doi.org/10.2337/dc17-0921>.
- 792 [5] Yates T, Zaccardi F, Dhalwani NN, Davies MJ, Bakrania K, Celis-Morales CA, et al. Association  
793 of walking pace and handgrip strength with all-cause, cardiovascular, and cancer mortality: a UK  
794 Biobank observational study. *European Heart Journal* 2017;38:3232–40.  
795 <https://doi.org/10.1093/eurheartj/ehx449>.
- 796 [6] Soltanisarvestani M, Lynskey N, Gray S, Gill JMR, Pell JP, Sattar N, et al. Associations of grip  
797 strength and walking pace with mortality in stroke survivors: A prospective study from UK  
798 Biobank. *Scandinavian Journal of Medicine & Science in Sports* 2023;33:1190–200.  
799 <https://doi.org/10.1111/sms.14352>.

- 800 [7] Nishita Y, Nakamura A, Kato T, Otsuka R, Iwata K, Tange C, et al. Links Between Physical Frailty  
801 and Regional Gray Matter Volumes in Older Adults: A Voxel-Based Morphometry Study. *J Am*  
802 *Med Dir Assoc* 2019;20:1587-1592.e7. <https://doi.org/10.1016/j.jamda.2019.09.001>.
- 803 [8] Vaishya R, Misra A, Vaish A, Ursino N, D'Ambrosi R. Hand grip strength as a proposed new vital  
804 sign of health: a narrative review of evidences. *Journal of Health, Population and Nutrition*  
805 2024;43:7. <https://doi.org/10.1186/s41043-024-00500-y>.
- 806 [9] Zheng H, He Q, Xu H, Zheng X, Gu Y. Lower grip strength and insufficient physical activity can  
807 increase depressive symptoms among middle-aged and older European adults: a longitudinal  
808 study. *BMC Geriatrics* 2022;22:696. <https://doi.org/10.1186/s12877-022-03392-x>.
- 809 [10] Ganipineni VDP, Idavalapati ASKK, Tamalapakula SS, Moparthi V, Potru M, Owolabi OJ.  
810 Depression and Hand-Grip: Unraveling the Association. *Cureus* n.d.;15:e38632.  
811 <https://doi.org/10.7759/cureus.38632>.
- 812 [11] Zaccagni L, Toselli S, Bramanti B, Gualdi-Russo E, Mongillo J, Rinaldo N. Handgrip Strength in  
813 Young Adults: Association with Anthropometric Variables and Laterality. *Int J Environ Res Public*  
814 *Health* 2020;17:4273. <https://doi.org/10.3390/ijerph17124273>.
- 815 [12] Tscherpel C, Dern S, Hensel L, Ziemann U, Fink GR, Grefkes C. Brain responsivity provides an  
816 individual readout for motor recovery after stroke. *Brain* 2020;143:1873.  
817 <https://doi.org/10.1093/brain/awaa127>.
- 818 [13] Bonkhoff AK, Rehme AK, Hensel L, Tscherpel C, Volz LJ, Espinoza FA, et al. Dynamic  
819 connectivity predicts acute motor impairment and recovery post-stroke. *Brain Commun*  
820 2021;3:fcab227. <https://doi.org/10.1093/braincomms/fcab227>.
- 821 [14] McGrath R, Johnson N, Klawitter L, Mahoney S, Trautman K, Carlson C, et al. What are the  
822 association patterns between handgrip strength and adverse health conditions? A topical review.  
823 *SAGE Open Medicine* 2020;8:2050312120910358. <https://doi.org/10.1177/2050312120910358>.
- 824 [15] Wunderle V, Kuzu TD, Tscherpel C, Fink GR, Grefkes C, Weiss PH. Age- and sex-related changes  
825 in motor functions: a comprehensive assessment and component analysis. *Front Aging Neurosci*  
826 2024;16. <https://doi.org/10.3389/fnagi.2024.1368052>.
- 827 [16] de Araújo Amaral C, Amaral TLM, Monteiro GTR, de Vasconcellos MTL, Portela MC. Factors  
828 associated with low handgrip strength in older people: data of the Study of Chronic Diseases  
829 (Edoc-I). *BMC Public Health* 2020;20:395. <https://doi.org/10.1186/s12889-020-08504-z>.
- 830 [17] Pua Y-H, Tay L, Clark RA, Thumboo J, Tay E-L, Mah S-M, et al. Associations of height, weight,  
831 and body mass index with handgrip strength: A Bayesian comparison in older adults. *Clinical*  
832 *Nutrition ESPEN* 2023;54:206–10. <https://doi.org/10.1016/j.clnesp.2023.01.028>.
- 833 [18] Bhattacharjee B, Ghosh J, Bhattacharjee A, Singh K, Roychowdhury S, Roy A, et al. Association  
834 of handgrip strength with blood pressure, waist hip ratio, visceral adiposity index, C-reactive  
835 protein among adult population of Kolkata: A hospital based cross-sectional observational study.  
836 *Clinical Nutrition ESPEN* 2023;58:523. <https://doi.org/10.1016/j.clnesp.2023.09.291>.
- 837 [19] Agtuahene MA, Quartey J, Kwakye S. Influence of hand dominance, gender, and body mass index  
838 on hand grip strength. *S Afr J Physiother* 2023;79:1923. <https://doi.org/10.4102/sajp.v79i1.1923>.
- 839 [20] Chandrasekaran B, Ghosh A, Prasad C, Krishnan K, Chandrasharma B. Age and Anthropometric  
840 Traits Predict Handgrip Strength in Healthy Normals. *J Hand Microsurg* 2016;02:58–61.  
841 <https://doi.org/10.1007/s12593-010-0015-6>.
- 842 [21] Vianna L, Oliveira R, Araujo CG. Age-Related Decline in Handgrip Strength Differs According  
843 to Gender. *Journal of Strength and Conditioning Research / National Strength & Conditioning*  
844 *Association* 2007;21:1310–4. <https://doi.org/10.1519/R-23156.1>.
- 845 [22] Kim J, Kim Y, Oh JW, Lee S. Sex differences of the association between handgrip strength and  
846 health-related quality of life among patients with cancer. *Sci Rep* 2024;14:9876.  
847 <https://doi.org/10.1038/s41598-024-60710-6>.

- 848 [23] Komeyer V, Eickhoff SB, Grefkes C, Patil KR, Raimondo F. A framework for confounder  
849 considerations in AI-driven precision medicine 2024:2024.02.02.24302198.  
850 <https://doi.org/10.1101/2024.02.02.24302198>.
- 851 [24] Spruit MA, Sillen MJH, Groenen MTJ, Wouters EFM, Franssen FME. New normative values for  
852 handgrip strength: results from the UK Biobank. *J Am Med Dir Assoc* 2013;14:775.e5-11.  
853 <https://doi.org/10.1016/j.jamda.2013.06.013>.
- 854 [25] Rehme AK, Fink GR, von Cramon DY, Grefkes C. The Role of the Contralesional Motor Cortex  
855 for Motor Recovery in the Early Days after Stroke Assessed with Longitudinal fMRI. *Cerebral*  
856 *Cortex* 2011;21:756–68. <https://doi.org/10.1093/cercor/bhq140>.
- 857 [26] Hwang J, Lee J, Lee K-S. A deep learning-based method for grip strength prediction: Comparison  
858 of multilayer perceptron and polynomial regression approaches. *PLoS One* 2021;16:e0246870.  
859 <https://doi.org/10.1371/journal.pone.0246870>.
- 860 [27] Allen N, Sudlow C, Downey P, Peakman T, Danesh J, Elliott P, et al. UK Biobank: Current status  
861 and what it means for epidemiology. *Health Policy and Technology* 2012;1:123–6.  
862 <https://doi.org/10.1016/j.hlpt.2012.07.003>.
- 863 [28] Collins R. UK Biobank: protocol for a large-scale prospective epidemiological resource. 2007.  
864 <http://www.ukbiobank.ac.uk/wp-content/uploads/2011/11/UKBiobank-Protocol.pdf> (21 March  
865 2017). n.d.
- 866 [29] UK Biobank. Algorithmically defined outcomes (ADOs) 2022.  
867 <https://biobank.ndph.ox.ac.uk/showcase/refer.cgi?id=460> (accessed June 20, 2024).
- 868 [30] UK Biobank. First Occurrence of Health Outcomes 2019.  
869 <https://biobank.ndph.ox.ac.uk/showcase/refer.cgi?id=593> (accessed August 1, 2024).
- 870 [31] Glanville KP, Coleman JRI, Howard DM, Pain O, Hanscombe KB, Jermy B, et al. Multiple  
871 measures of depression to enhance validity of major depressive disorder in the UK Biobank.  
872 *BJPsych Open* 2021;7:e44. <https://doi.org/10.1192/bjo.2020.145>.
- 873 [32] Firth J, Stubbs B, Vancampfort D, Firth JA, Large M, Rosenbaum S, et al. Grip Strength Is  
874 Associated With Cognitive Performance in Schizophrenia and the General Population: A UK  
875 Biobank Study of 476559 Participants. *Schizophr Bull* 2018;44:728–36.  
876 <https://doi.org/10.1093/schbul/sby034>.
- 877 [33] Bobos P, Nazari G, Lu Z, MacDermid JC. Measurement Properties of the Hand Grip Strength  
878 Assessment: A Systematic Review With Meta-analysis. *Arch Phys Med Rehabil* 2020;101:553–  
879 65. <https://doi.org/10.1016/j.apmr.2019.10.183>.
- 880 [34] Petersen P, Petrick M, Connor H, Conklin D. Grip Strength and Hand Dominance: Challenging  
881 the 10% Rule. *The American Journal of Occupational Therapy* 1989;43:444–7.  
882 <https://doi.org/10.5014/ajot.43.7.444>.
- 883 [35] Gómez-Campos R, Vidal Espinoza R, de Arruda M, Ronque ERV, Urra-Albornoz C, Minango JC,  
884 et al. Relationship between age and handgrip strength: Proposal of reference values from infancy  
885 to senescence. *Front Public Health* 2023;10. <https://doi.org/10.3389/fpubh.2022.1072684>.
- 886 [36] Hamdan S, More S, Sasse L, Komeyer V, Patil KR, Raimondo F. Julearn: an easy-to-use library  
887 for leakage-free evaluation and inspection of ML models 2023.  
888 <https://doi.org/10.48550/arXiv.2310.12568>.
- 889 [37] Pedregosa F, Varoquaux G, Gramfort A, Michel V, Thirion B, Grisel O, et al. Scikit-learn:  
890 Machine Learning in Python. *Journal of Machine Learning Research* 2011;12:2825–30.
- 891 [38] R: Fast Heuristics For The Estimation Of the C Constant Of A... n.d. [https://search.r-](https://search.r-project.org/CRAN/refmans/LiblineaR/html/heuristicC.html)  
892 [project.org/CRAN/refmans/LiblineaR/html/heuristicC.html](https://search.r-project.org/CRAN/refmans/LiblineaR/html/heuristicC.html) (accessed June 9, 2024).
- 893 [39] Young DS. *Handbook of Regression Methods*. New York: Chapman and Hall/CRC; 2017.  
894 <https://doi.org/10.1201/9781315154701>.
- 895 [40] Beheshti I, Nugent S, Potvin O, Duchesne S. Bias-adjustment in neuroimaging-based brain age  
896 frameworks: A robust scheme. *NeuroImage: Clinical* 2019;24:102063.  
897 <https://doi.org/10.1016/j.nicl.2019.102063>.

- 898 [41] Lin LI. A concordance correlation coefficient to evaluate reproducibility. *Biometrics*  
899 1989;45:255–68.
- 900 [42] Sudlow C, Gallacher J, Allen N, Beral V, Burton P, Danesh J, et al. UK biobank: an open access  
901 resource for identifying the causes of a wide range of complex diseases of middle and old age.  
902 *PLoS Med* 2015;12:e1001779. <https://doi.org/10.1371/journal.pmed.1001779>.
- 903 [43] Miller KL, Alfaro-Almagro F, Bangerter NK, Thomas DL, Yacoub E, Xu J, et al. Multimodal  
904 population brain imaging in the UK Biobank prospective epidemiological study. *Nat Neurosci*  
905 2016;19:1523–36. <https://doi.org/10.1038/nn.4393>.
- 906 [44] Alfaro-Almagro F, Jenkinson M, Bangerter NK, Andersson JLR, Griffanti L, Douaud G, et al.  
907 Image processing and Quality Control for the first 10,000 brain imaging datasets from UK  
908 Biobank. *NeuroImage* 2018;166:400–24. <https://doi.org/10.1016/j.neuroimage.2017.10.034>.
- 909 [45] Halchenko YO, Meyer K, Poldrack B, Solanky DS, Wagner AS, Gors J, et al. DataLad: distributed  
910 system for joint management of code, data, and their relationship. *Journal of Open Source Software*  
911 2021;6:3262. <https://doi.org/10.21105/joss.03262>.
- 912 [46] Wagner AS, Waite LK, Wierzbka M, Hoffstaedter F, Waite AQ, Poldrack B, et al. FAIRly big: A  
913 framework for computationally reproducible processing of large-scale data. *Sci Data* 2022;9:80.  
914 <https://doi.org/10.1038/s41597-022-01163-2>.
- 915 [47] Schaefer A, Kong R, Gordon EM, Laumann TO, Zuo X-N, Holmes AJ, et al. Local-Global  
916 Parcellation of the Human Cerebral Cortex from Intrinsic Functional Connectivity MRI. *Cereb*  
917 *Cortex* 2018;28:3095–114. <https://doi.org/10.1093/cercor/bhx179>.
- 918 [48] Tian Y, Margulies DS, Breakspear M, Zalesky A. Topographic organization of the human  
919 subcortex unveiled with functional connectivity gradients. *Nat Neurosci* 2020;23:1421–32.  
920 <https://doi.org/10.1038/s41593-020-00711-6>.
- 921 [49] Diedrichsen J, Balsters JH, Flavell J, Cussans E, Ramnani N. A probabilistic MR atlas of the  
922 human cerebellum. *NeuroImage* 2009;46:39–46.  
923 <https://doi.org/10.1016/j.neuroimage.2009.01.045>.
- 924 [50] Zhao Q-Y, Luo J-C, Su Y, Zhang Y-J, Tu G-W, Luo Z. Propensity score matching with R:  
925 conventional methods and new features. *Ann Transl Med* 2021;9:812.  
926 <https://doi.org/10.21037/atm-20-3998>.
- 927 [51] Salkind NJ. *Encyclopedia of Research Design*. SAGE; 2010.
- 928 [52] Glass GV, Peckham PD, Sanders JR. Consequences of Failure to Meet Assumptions Underlying  
929 the Fixed Effects Analyses of Variance and Covariance. *Review of Educational Research*  
930 1972;42:237–88. <https://doi.org/10.3102/00346543042003237>.
- 931 [53] Harwell MR, Rubinstein EN, Hayes WS, Olds CC. Summarizing Monte Carlo Results in  
932 Methodological Research: The One- and Two-Factor Fixed Effects ANOVA Cases. *Journal of*  
933 *Educational Statistics* 1992;17:315–39. <https://doi.org/10.3102/10769986017004315>.
- 934 [54] Lumley T, Diehr P, Emerson S, Chen L. The importance of the normality assumption in large  
935 public health data sets. *Annu Rev Public Health* 2002;23:151–69.  
936 <https://doi.org/10.1146/annurev.publhealth.23.100901.140546>.
- 937 [55] Liao K-H. Hand Grip Strength in Low, Medium, and High Body Mass Index Males and Females.  
938 *Middle East J Rehabil Health Stud* 2016;3. <https://doi.org/10.17795/mejrh-33860>.
- 939 [56] Arvandi M, Strasser B, Meisinger C, Volaklis K, Gothe RM, Siebert U, et al. Gender differences  
940 in the association between grip strength and mortality in older adults: results from the KORA-age  
941 study. *BMC Geriatrics* 2016;16:201. <https://doi.org/10.1186/s12877-016-0381-4>.
- 942 [57] Hwang J, Lee J, Lee K-S. A deep learning-based method for grip strength prediction: Comparison  
943 of multilayer perceptron and polynomial regression approaches. *PLoS ONE* 2021;16:e0246870.  
944 <https://doi.org/10.1371/journal.pone.0246870>.
- 945 [58] Meysami S, Raji CA, Glatt RM, Popa ES, Ganapathi AS, Bookheimer T, et al. Handgrip Strength  
946 Is Related to Hippocampal and Lobar Brain Volumes in a Cohort of Cognitively Impaired Older

- 947 Adults with Confirmed Amyloid Burden. *J Alzheimers Dis* n.d.;91:999–1006.  
948 <https://doi.org/10.3233/JAD-220886>.
- 949 [59] Stenholm S, Harris TB, Rantanen T, Visser M, Kritchevsky SB, Ferrucci L. Sarcopenic obesity -  
950 definition, etiology and consequences. *Curr Opin Clin Nutr Metab Care* 2008;11:693–700.  
951 <https://doi.org/10.1097/MCO.0b013e328312c37d>.
- 952 [60] Stock R, Thrane G, Askim T, Anke A, Mork PJ. Development of grip strength during the first year  
953 after stroke. *J Rehabil Med* 2019;51:248–56. <https://doi.org/10.2340/16501977-2530>.
- 954 [61] Poggesi A, Insalata G, Papi G, Rinnoci V, Donnini I, Martini M, et al. Gender differences in post-  
955 stroke functional outcome at discharge from an intensive rehabilitation hospital. *European Journal*  
956 *of Neurology* 2021;28:1601–8. <https://doi.org/10.1111/ene.14769>.
- 957 [62] Trivedi MH. The Link Between Depression and Physical Symptoms. *Prim Care Companion J Clin*  
958 *Psychiatry* 2004;6:12–6.
- 959